



31

TECHNICAL NOTE

D-1389

FORCE-TEST INVESTIGATION OF THE STABILITY AND CONTROL
CHARACTERISTICS OF A FOUR-PROPELLER TILT-WING
VTOL MODEL WITH A PROGRAMED FLAP

By William A. Newsom, Jr.

Langley Research Center
Langley Station, Hampton, Va.

NATIONAL AERONAUTICS AND SPACE ADMINISTRATION
WASHINGTON

September 1962

NATIONAL AERONAUTICS AND SPACE ADMINISTRATION

TECHNICAL NOTE D-1389

FORCE-TEST INVESTIGATION OF THE STABILITY AND CONTROL
CHARACTERISTICS OF A FOUR-PROPELLER TILT-WING
VTOL MODEL WITH A PROGRAMED FLAP

By William A. Newsom, Jr.

SUMMARY

A wind-tunnel investigation has been made to determine the longitudinal and lateral stability and control characteristics of a model of a high-wing four-propeller, tilt-wing VTOL model. The model was equipped with a 35-percent-chord slotted flap which was programed to deflect as the wing rotated so that the flap was retracted for the 0° and 90° wing-incidence conditions and was deflected downward for intermediate angles of incidence to obtain favorable performance and longitudinal trim characteristics in the transitional flight range. Three different flap-aileron configurations were tested and the control effectiveness of the all-movable horizontal tail and the ailerons was also determined.

It was found that, by the use of a full-span flap and by proper programing of the horizontal-tail incidence, it would be possible to eliminate the variation of pitching-moment trim change during the transition. It was not possible, however, to accomplish the same result with a partial-span flap, even when the flap effectiveness was augmented by the use of drooped conventional ailerons and horizontal-tail deflection. It was also found that the slot-lip aileron used in conjunction with the full-span flap did not provide satisfactory control, particularly because it was almost totally ineffective for yaw control in the hovering condition. Tests of the conventional ailerons used in conjunction with the partial-span flap and previous tests of the effectiveness of a full-span aileron indicated that a more effective control could be obtained by actuating the full-span flap itself as an aileron or by using the rearward portion of the flap as an aileron.

INTRODUCTION

In the past, tests of various tilt-wing VTOL airplane models have shown that such configurations characteristically tend to develop a large nose-up pitching moment as the aircraft starts through transition

from hovering to forward flight. (See refs. 1 and 2.) This change in pitch trim with speed and wing incidence can severely limit the range of center-of-gravity positions for which it is possible to perform the transition successfully. Force tests of tilt-wing-flap combinations, such as those of references 3 and 4, have indicated that with proper programing of flap deflection with the wing tilt it is possible to design a tilt-wing VTOL aircraft which has essentially no longitudinal trim change throughout the transition from hovering to normal unstalled forward flight and that such a configuration would also have favorable performance characteristics.

An investigation has therefore been made of the stability and control characteristics of a model of a tilt-wing vertical take-off-and-landing high-wing transport airplane having a slotted flap programed to deflect as the wing tilts from 90° for hovering to 0° for forward flight. The flap programing was arranged so that the flap was retracted for the 90° and 0° incidence conditions to give a clean configuration for hovering and normal forward flight, and the flap was deflected for intermediate angles of incidence to obtain favorable performance and longitudinal trim characteristics for the transition flight conditions. The results of the flight tests of the model are reported in reference 5, and the results of the force tests are presented in this paper.

The force tests included measurement of the aerodynamic characteristics in transition and normal forward flight for three different flap-aileron configurations. The control effectiveness of the all-movable horizontal tail and the ailerons was obtained for the full range of wing incidence tested (80° to 0°). All transition tests were made for the condition of steady level flight or zero forward acceleration.

SYMBOLS

The forces and moments are based on the stability-axis system, which is an orthogonal system with the origin at the airplane center of gravity. The Z-axis is in the plane of symmetry and perpendicular to the relative wind, the X-axis is in the plane of symmetry and perpendicular to the Z-axis, and the Y-axis is perpendicular to the plane of symmetry.

b	wing span, ft
C_D	drag coefficient, F_D/qS
C_L	lift coefficient, F_L/qS
C_l	rolling-moment coefficient, M_X/qSb

C_m	pitching-moment coefficient, $M_Y/qS\bar{c}$
C_n	yawing-moment coefficient, M_Z/qSb
C_Y	side-force coefficient, F_Y/qS
\bar{c}	wing mean aerodynamic chord, ft
F_D	drag, lb
F_L	lift, lb
F_Y	side force, lb
i_t	horizontal-tail incidence, positive when trailing edge is down, deg
i_w	wing incidence, deg
M_X	rolling moment, ft-lb
$M_{X\beta} = \frac{\partial M_X}{\partial \beta}$	
M_Y	pitching moment, ft-lb
$M_{Y\alpha} = \frac{\partial M_Y}{\partial \alpha}$	
M_Z	yawing moment, ft-lb
$M_{Z\beta} = \frac{\partial M_Z}{\partial \beta}$	
q	free-stream dynamic pressure, lb/sq ft
S	wing area, sq ft
V	velocity, ft/sec
X, Y, Z	coordinate axes
α	angle of attack of fuselage, deg

β	angle of sideslip, deg
$\delta_{a'R}$	deflection of right aileron, positive when trailing edge is down, deg

MODEL

The model used in the investigation was the model of a tilt-wing VTOL transport used in the flight-test investigation of reference 5. Figure 1 shows a three-view drawing and a photograph of the model and table I presents the geometric characteristics. The model had four 3-blade propellers each of which was powered by an air motor. The propellers were not interconnected but the motors were all connected to a common manifold and a valve was provided on each motor inlet by which the motor speeds could be synchronized, if necessary, before a test. Calibrations showed, however, that the motors stayed in synchronization so well that it was only necessary to readjust the speed of a motor after it had been disassembled for maintenance. The speed of the motors was changed to vary the thrust of the propellers. The propeller blade angle was 16° at 0.75 radius and the direction of rotation was as shown in figure 1.

The wing was pivoted at the 65-percent-chord station and could be rotated between incidences of 0° and 90° . As the wing incidence changed, the 35-percent-chord slotted flap was programmed to deflect as shown in figure 2. The model had an all-movable horizontal tail and conventional rudder controls for forward flight. Two types of ailerons were used during the model tests. The original model configuration as shown in figure 1 had a conventional aileron which was used in conjunction with a partial-span single-slotted flap. A second type of aileron was installed on the model after, as a result of early tests, the slotted flap had been extended to full span. (See fig. 1.) A slot-lip aileron was created by hinging the outer 30-percent span of each slot lip. A typical cross section of the wing through the slot-lip aileron is shown in figure 3.

TESTS

The tests were made in the Langley full-scale tunnel with the model mounted on a support strut near the lower edge of the entrance cone and about 5 feet above a groundboard. An electric strain-gage balance was used to measure the forces and moments. All the tests were made at a condition of zero forward acceleration by adjusting the tunnel speed

and model power for each wing incidence (fuselage $\alpha = 0^\circ$) until the drag trim point was reached.

Three different flap-aileron configurations were tested: partial-span slotted flap with 30-percent-span conventional ailerons, partial-span slotted flap with 30-percent-span conventional ailerons drooped 20° , and a full-span slotted flap with 30-percent-span slot-lip ailerons. With the test condition set as mentioned above (drag trimmed at fuselage $\alpha = 0^\circ$), the angle of attack was varied for longitudinal stability and control tests from -10° to 20° with the horizontal tail off and with the horizontal tail set at various angles of incidence from -10° to 30° . For the full-span-flap configuration, a test was made of the variation of rolling moment, yawing moment, and side force over a range of sideslip angles from -20° to 20° for each angle of wing incidence from 0° to 80° . Aileron control effectiveness was measured at $\beta = 0^\circ$ for all flap-aileron configurations.

The tests at wing incidences of 0° , 10° , and 20° were made at an airspeed of about 23 knots which gave an effective Reynolds number based on the wing chord and free-stream velocity of about 200,000. For the tests at higher angles of wing incidence, it was necessary to reduce the tunnel airspeed below 23 knots to avoid exceeding the model motor limitations.

RESULTS AND DISCUSSION

The results of a force-test investigation to determine the aerodynamic characteristics of a model of a tilt-wing VTOL transport with a programed flap are presented with the moments based on the center-of-gravity positions shown in figure 4. These were the actual center-of-gravity positions of the model as it was flown during the tests described in reference 5. The data for the normal forward flight tests ($i_w = 0^\circ$ and 10°) are presented in coefficient form, but since the coefficients approach infinity and become essentially meaningless as the velocity approaches zero, the data for the transition tests ($i_w = 20^\circ$ to 80°) have been scaled up to the model flying weight of 51.28 pounds. This scaling of the data is accomplished by determining the factor required to make the lift equal to the desired value (51.28 pounds, which was the weight of the model during the flight tests of ref. 5) and multiplying all forces and moments by the factor. The corresponding test velocities are scaled up by the square root of the factor.

Longitudinal Stability and Control

The data for the configuration having a partial-span slotted flap and a 30-percent-span conventional aileron (with the ailerons not drooped) are presented in figures 5 and 6.

In figure 5 are plots presenting the variation of lift, drag, and pitching moment with angle of attack at several horizontal-tail deflections as well as for the horizontal-tail-off condition. The stability and trim characteristics from these data are summarized in figure 6. For the tail-on case, the stability parameter $M_{Y\alpha}$ was measured at $\alpha = 0^\circ$ with the tail incidence needed to give zero pitching moment whenever possible. In cases where it was not possible to get zero pitching moment, the effect of tail incidence on $M_{Y\alpha}$ was virtually negligible and some average slope was used. At angles of wing incidence from 90° to 60° the model was neutrally stable tail off and the addition of the horizontal tail did not increase the stability, because of the low dynamic pressure. At lower angles of wing incidence the model became unstable with the tail off but, because of the higher dynamic pressure, the addition of a horizontal tail made the model stable. The figure also shows that, at angles of wing incidence from 80° to 40° , the model has a nose-up pitching moment which cannot be trimmed with the horizontal tail. An analysis of the curves shows that for the worst condition ($i_w = 60^\circ$) the model would require an upward force of about 2 percent of the model weight from some auxiliary control device at the tail which seems to be a very significant amount.

The longitudinal data for the configuration having a partial-span slotted flap and a 30-percent-span conventional aileron with the ailerons drooped 20° are presented in figures 7 and 8. Figure 7 presents the variation of lift, drag, and pitching moment with angle of attack for several horizontal-tail deflections and for horizontal tail off, and a summary plot showing stability and trim characteristics extracted from this basic data is presented as figure 8. The point of these tests was to determine quantitatively the effect of the drooped ailerons in alleviating the trim problem at high angles of incidence since the flight tests of reference 5 had shown qualitatively that this procedure was not effective in eliminating the pitching trim problem. Comparison of the data from the summary figure (fig. 8) with that of the corresponding figure 6 shows that even though the nose-up pitching moments measured at wing incidences above and below the critical range near 60° incidence were reduced, the pitching moment near 60° wing incidence was still as bad as for the previous configuration which had undrooped ailerons. The longitudinal stability and the horizontal-tail effectiveness were little changed by the change in aileron configuration.

The longitudinal data for the full-span-flap configuration are presented in figures 9 and 10. Figure 9 presents the variation of lift, drag, and pitching moment with angle of attack for several horizontal-tail deflections, and for horizontal tail off, for each angle of wing incidence. The longitudinal stability and trim characteristics measured from these basic data are summarized in figure 10. These data show that, when the model was fitted with the full-span slotted flap, the pitching moment in the critical range near $i_w = 50^\circ$ or 60° was reduced to the point where it was almost trimmed by use of the horizontal tail even though at such low speeds the tail has little effectiveness. In fact, analysis of the data of figure 9(d) indicates that the pitching moment in this most critical condition could probably have been trimmed by the use of a higher tail incidence of about 35° . For this full-span-flap configuration the longitudinal stability was little changed from that of the other configurations.

Lateral Stability and Control

Figure 11 shows the effectiveness of the aileron throughout the wing incidence range for the partial-span-flap configuration with undrooped conventional ailerons. Qualitatively, these data show the results that would be expected; that is, that the ailerons produce principally yawing moments in hovering flight and rolling moments in forward flight. One point that bears further study is the magnitudes of the yawing moments produced in hovering flight. Inspection of figure 11 shows that at $i_w = 80^\circ$, $\pm 20^\circ$ deflection of both ailerons would give a yawing moment of ± 10 foot-pounds. This value would correspond to a force of approximately ± 2.5 pounds at the tail jet which was approximately the force used in the flight tests of reference 5 for hovering in still air. A better indication of the suitability of these ailerons for yaw control in hovering might be obtained by a comparison of the control power of these ailerons with that required in the handling requirements for these airplanes. In this case if the model is a dynamically scaled model in the range from $1/5$ to $1/10$ scale, the yaw control power of the ailerons would be only about one-fourth to one-third of that indicated as being required by reference 6.

Figure 12 shows the effectiveness of the aileron for the partial-span-flap drooped-aileron configuration. These data show the expected result in that, as the ailerons are deflected downward from the 20° drooped position, they tend to lose their effectiveness in producing rolling moments at the low angles of incidence or yawing moments at the high angles of incidence.

The effectiveness of the slot-lip aileron used with the full-span flap is shown by the data of figure 13. There seem to be two important

points to note. First, the slot-lip aileron would not be usable as a yaw control in hovering since it does not produce any yawing moment as indicated by the data for the near hovering condition of $i_w = 80^\circ$. Second, in the normal forward-flight conditions as represented by the $i_w = 0^\circ$ and 10° tests the slot-lip ailerons produce only about one-third of the rolling moment of the conventional ailerons. (See fig. 11.) It would seem that a more satisfactory system for providing aileron control would be to actuate the entire full-span flap as an aileron or to actuate the rearward portion of the flap. The effectiveness of such a full-span aileron is shown in reference 7.

The data of figure 14 show the variation of rolling moment, yawing moment, and side force with sideslip angle, and these data are summarized in figure 15 in terms of the directional stability parameter $M_{Z\beta}$ and the effective dihedral parameter $M_{X\beta}$. The plots of rolling moment and yawing moment in figure 14 are, as in other lateral data figures, to some degree erratic. It is believed that, in general, the erratic data are due in part to random gusts in the tunnel and wing stalling which can cause large changes in some of the moments. For example, a rolling moment of about 1.5 foot-pounds, which is representative of the scatter in the data, can be produced by a difference in lift of 1 pound, which is only 2 percent of the total lift, distributed over one semispan. In this connection, a tuft survey showed that there was a severe stall over the wing center section which at times, possibly due to wing asymmetry, extended over the inboard portion of the right wing. The plots of rolling-moment variation with sideslip are extremely unsymmetrical, but seem to show, in general, the trends indicated by the slopes $M_{X\beta}$ presented in figure 15.

The directional stability data show, in general, that the model was unstable in the low-speed portion of the transition range and that it was stable at higher speeds where the wing incidence was less than 30° . Actually, the directional instability shown is very small; for example, at $i_w = 50^\circ$ which was the worst condition, $M_{Z\beta} = 0.3$ to 0.2 ft-lb/deg. This value is small compared with the 10 foot-pounds which was available from the tail-jet reaction yaw control used on the model.

SUMMARY OF RESULTS

The following results were obtained from the investigation of the static stability and control characteristics of a four-propeller tilt-wing VTOL model having a single slotted flap programed to deflect as the wing rotates.

1. For the full-span-flap configuration, the variation of trim pitching moment throughout the transition range was small for the tail-off condition with the particular flap programing built into the model.

2. With the horizontal tail fixed at low angles of incidence, the model experienced large nose-up pitching moments during the transition because of the download on the tail induced by the downwash from the wing.

3. By properly programing the horizontal-tail incidence to vary with wing incidence, it would be possible to reduce the pitching-moment variation through the transition range to zero or to a very low level.

4. It was not possible with a partial-span flap (even when augmented by drooped ailerons and horizontal-tail deflection) to eliminate the nose-up pitching moments encountered in the transition range.

5. The tests show that the slot-lip aileron tested in conjunction with the full-span flap did not provide satisfactory control. Specifically, it was almost totally ineffective as a yaw control for the hovering condition and was about one-third as effective for roll control in forward flight as were the conventional ailerons tested.

6. Tests of the conventional ailerons used with the partial-span flap and previous tests of the effectiveness of a full-span aileron indicated that a more effective control could be obtained by actuating the full-span flap itself as an aileron or by using the rearward portion of the flap as an aileron.

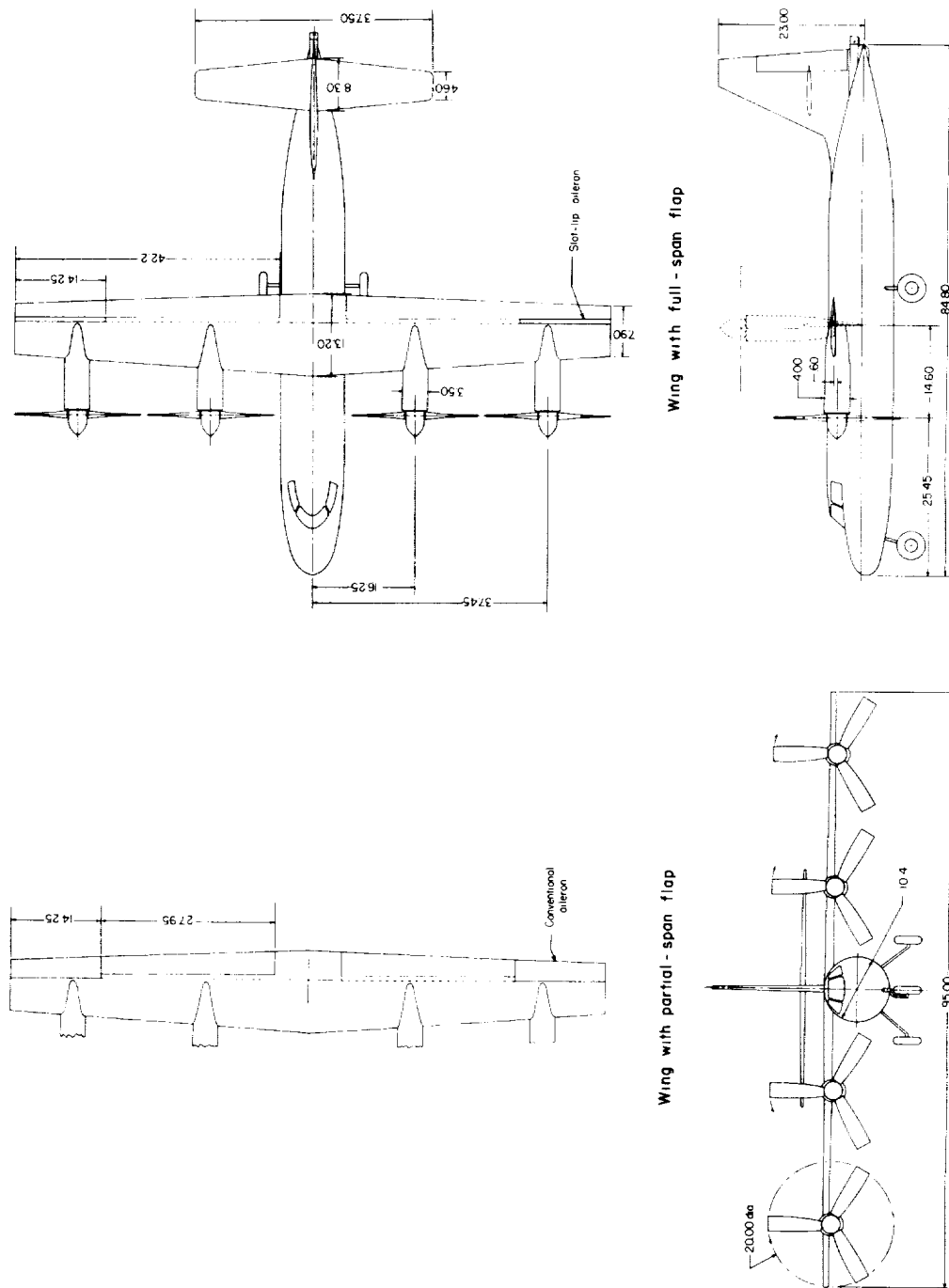
Langley Research Center,
National Aeronautics and Space Administration,
Langley Station, Hampton, Va., June 7, 1962.

REFERENCES

1. Tosti, Louis P.: Flight Investigation of Stability and Control Characteristics of a 1/8-Scale Model of a Tilt-Wing Vertical-Take-Off-And-Landing Airplane. NASA TN D-45, 1960.
2. Tosti, Louis P.: Flight Investigation of the Stability and Control Characteristics of a 1/4-Scale Model of a Tilt-Wing Vertical-Take-Off-And-Landing Aircraft. NASA MEMO 11-4-58L, 1959.
3. Newsom, William A., Jr.: Effect of Propeller Location and Flap Deflection on the Aerodynamic Characteristics of a Wing-Propeller Combination for Angles of Attack From 0° to 80° . NACA TN 3917, 1957.
4. Kuhn, Richard E., and Hayes, William C., Jr.: Wind-Tunnel Investigation of Longitudinal Aerodynamic Characteristics of Three Propeller-Driven VTOL Configurations in the Transition Speed Range, Including Effects of Ground Proximity. NASA TN D-55, 1960.
5. Newsom, William A., Jr.: Flight Investigation of the Longitudinal Stability and Control Characteristics of a Four-Propeller Tilt-Wing VTOL Model With a Programed Flap. NASA TN D-1390, 1962.
6. Tapscott, Robert J.: Helicopters and VTOL Aircraft - Criteria for Control and Response Characteristics in Hovering and Low-Speed Flight. Aero/Space Eng., vol. 19, no. 6, June 1960, pp. 38-41.
7. Newsom, William A., Jr.: Experimental Investigation of the Lateral Trim of a Wing-Propeller Combination at Angles of Attack up to 90° With All Propellers Turning in the Same Direction. NACA TN 4190, 1958.

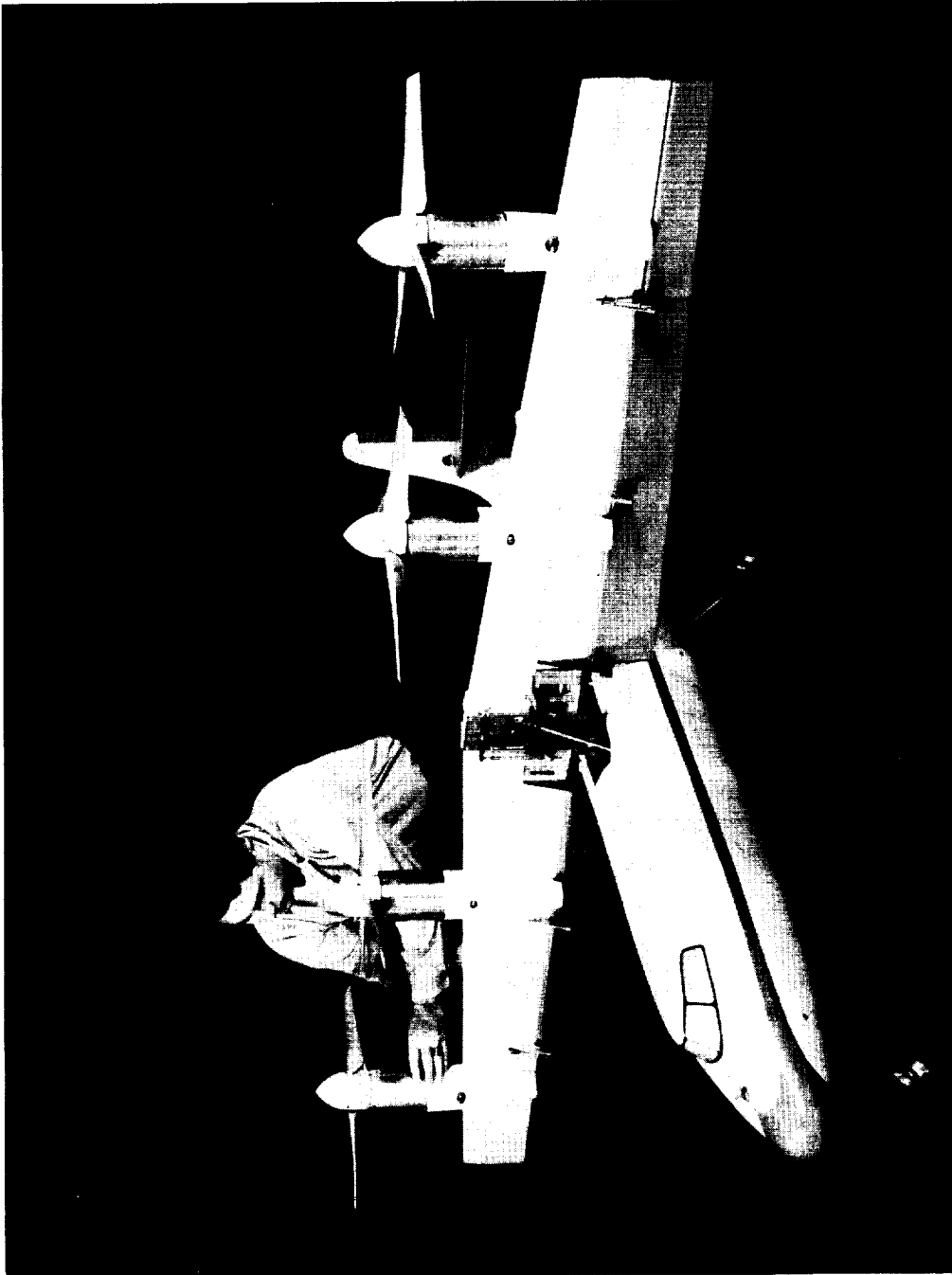
TABLE I.- GEOMETRIC CHARACTERISTICS OF MODEL

Fuselage:	
Length, in.	84.8
Diameter (maximum), in.	10.4
Wing:	
Area, sq in.	1,002.25
Aspect ratio	9
Mean aerodynamic chord, in.	10.77
Airfoil section	NACA 65-210
Tip chord, in.	7.9
Root chord, in.	13.2
Span, in.	95
Taper ratio	0.6
Sweepback of 0.65 chord	0
Dihedral angle, deg	0
Pivot station, percent chord	65
Flap chord, percent wing chord	35
Aileron, conventional (each):	
Chord, percent wing chord	35
Span, percent wing semispan	30
Aileron, slot-lip (each):	
Chord, in.	0.75
Span, percent wing semispan	30
Vertical tail:	
Area (total to center line), sq in.	269
Aspect ratio	1.97
Airfoil section	NACA 0009
Tip chord, in.	5.4
Root chord (at center line), in.	18.0
Span, in.	23.0
Taper ratio	0.3
Sweepback (leading edge), deg	25
Rudder (hinge line perpendicular to fuselage center line):	
Tip chord, in.	2.5
Root chord, in.	4.05
Span, in.	14.03
Horizontal tail:	
Area, sq in.	241.9
Aspect ratio	5.81
Airfoil section	NACA 0009
Tip chord, in.	4.60
Root chord, in.	8.3
Span, in.	37.5
Taper ratio	0.55
Sweepback (leading edge), deg	7.3
Mean aerodynamic chord, in.	6.62
Propellers (three blades each):	
Diameter, in.	20
Chord, in.	2.5
Solidity	0.239



(a) Sketch of model. All dimensions are in inches.

Figure 1.- Model used in tests.



(b) Photograph of model.

L-57-4940.1

Figure 1.- Concluded.

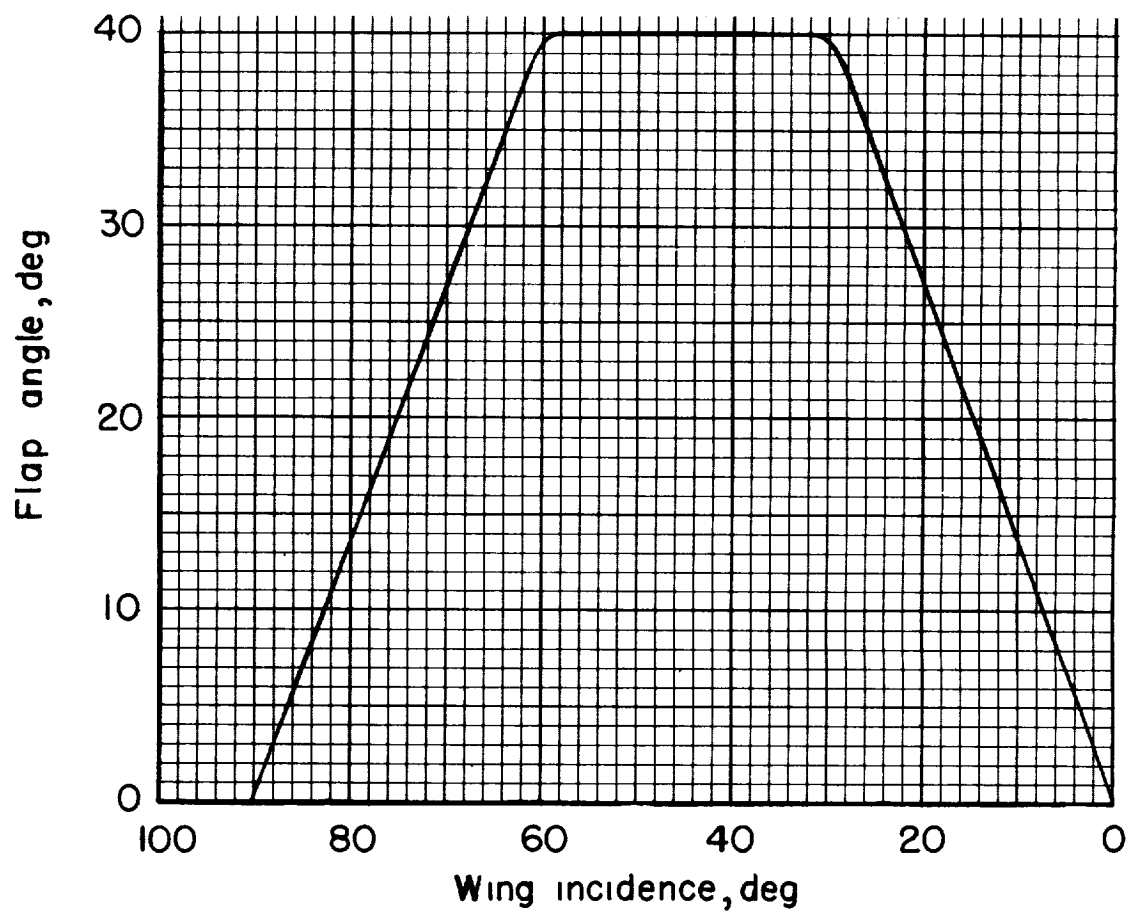


Figure 2.- Variation of model flap angle with wing incidence.

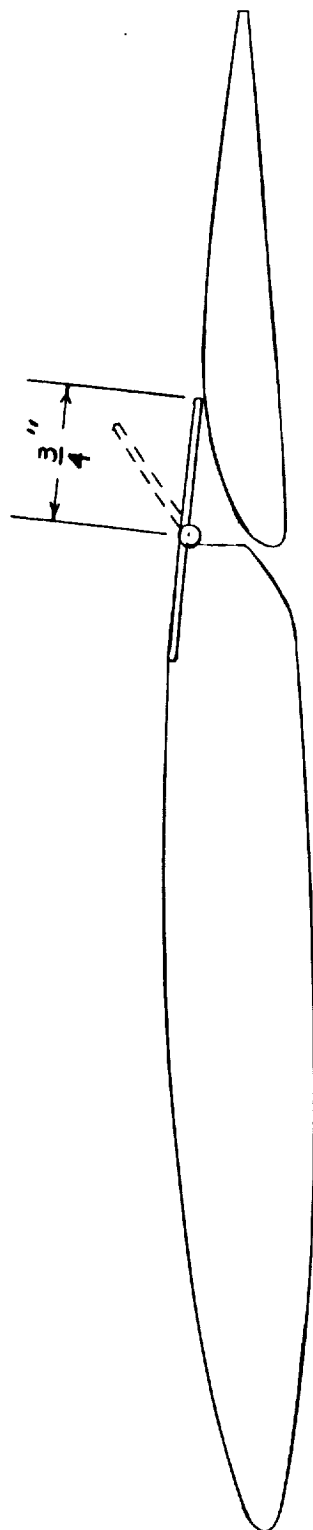


Figure 3.- Typical section through the slot-lip aileron.

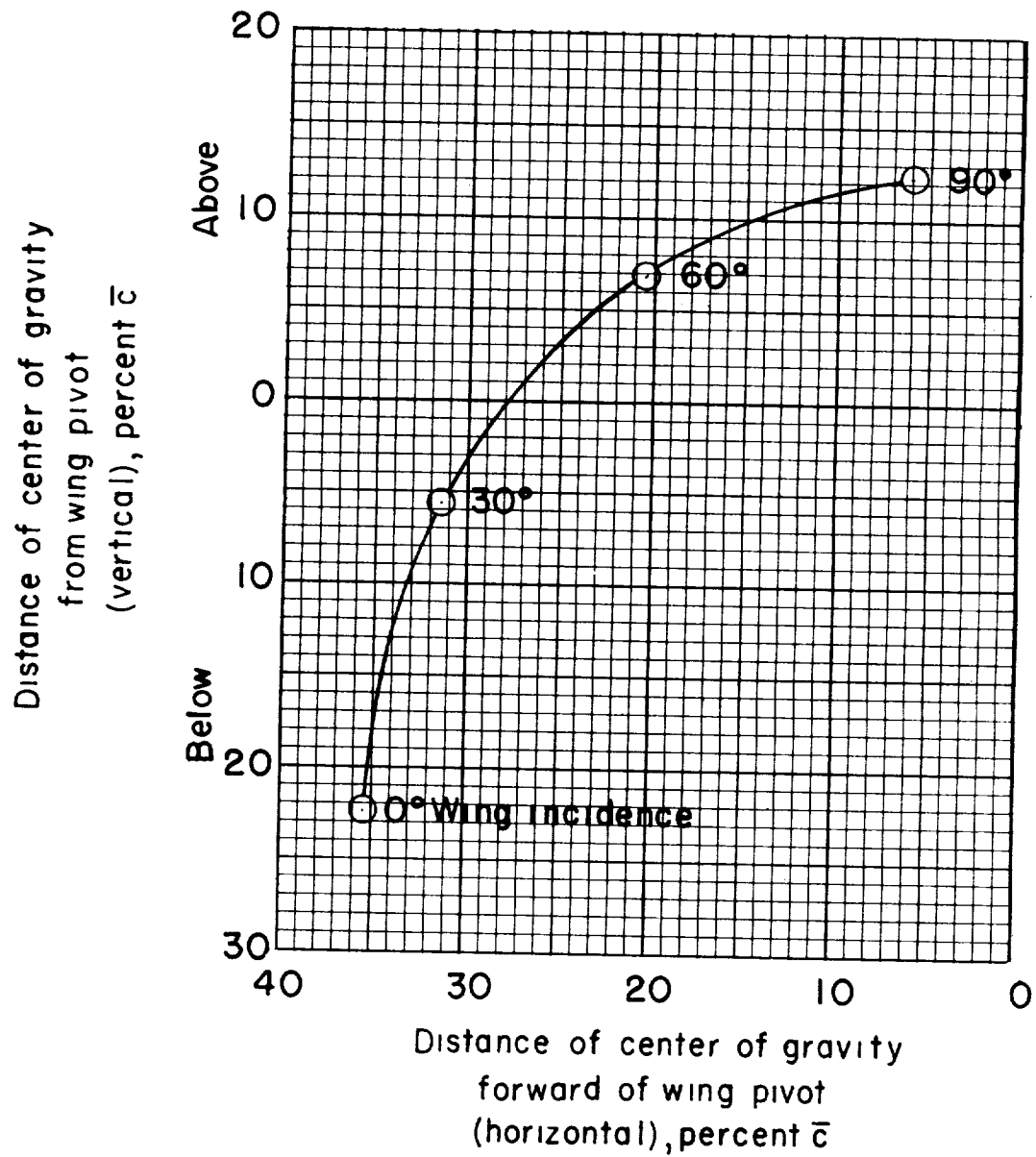
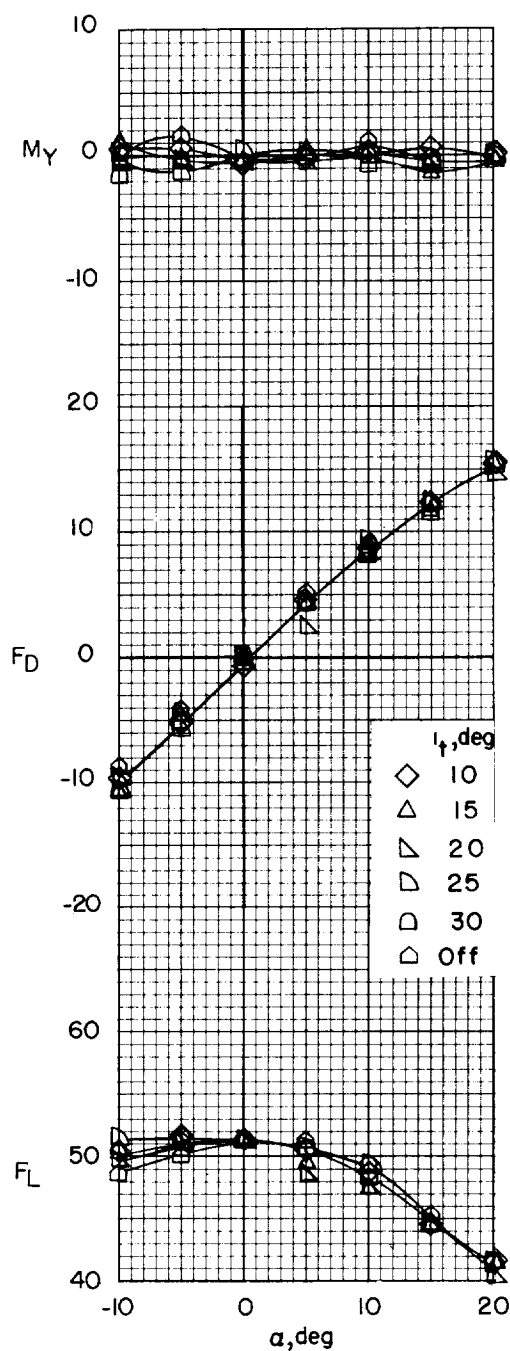
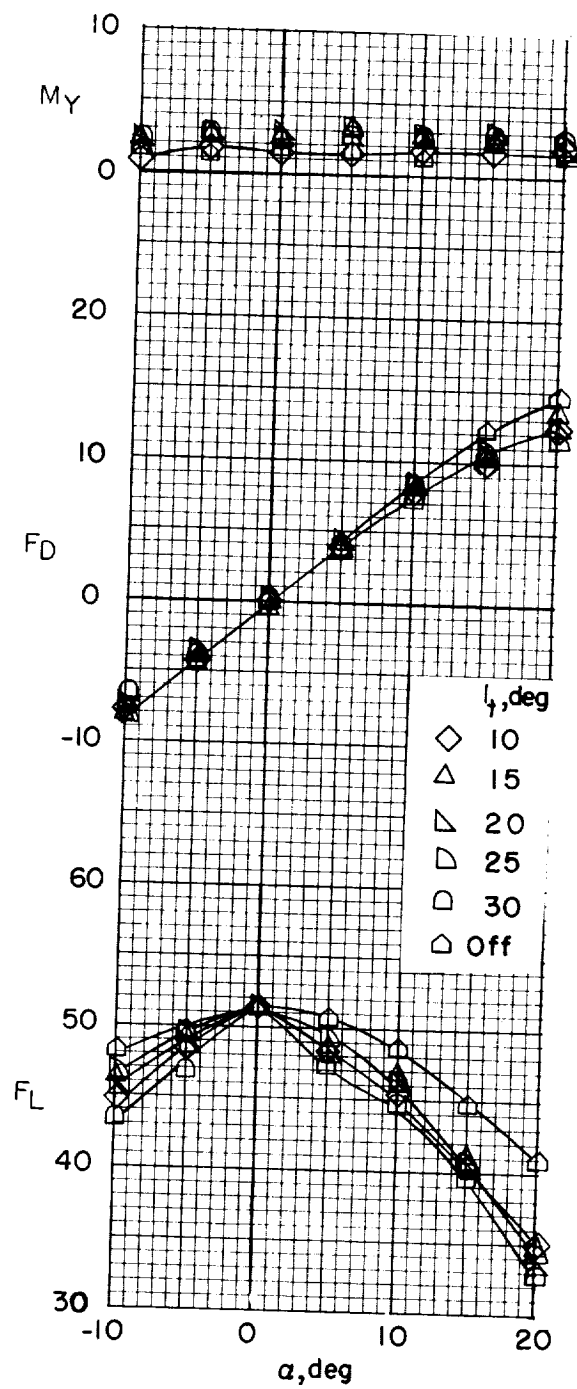


Figure 4.- Variation of model center of gravity with wing incidence.



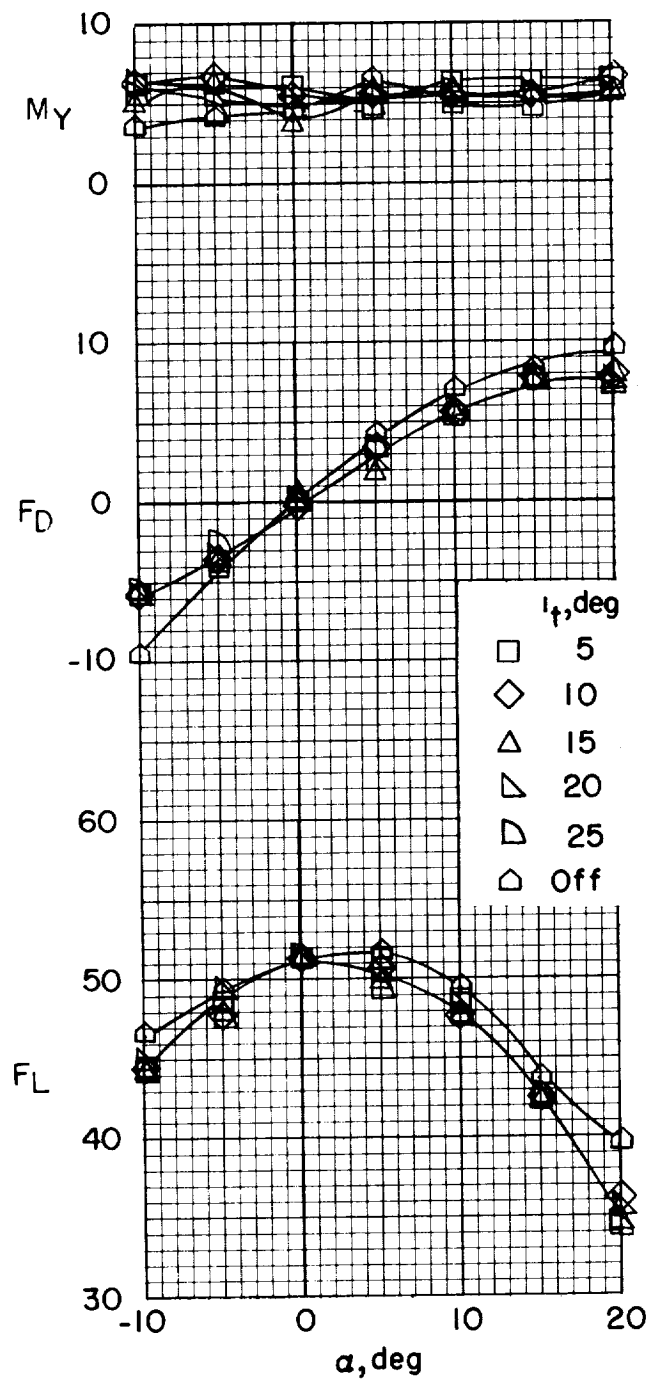
(a) $i_w = 80^\circ$; $V = 1.9$ feet per second.

Figure 5.- Longitudinal stability and control characteristics of the partial-span-flap configuration with undrooped conventional aileron.



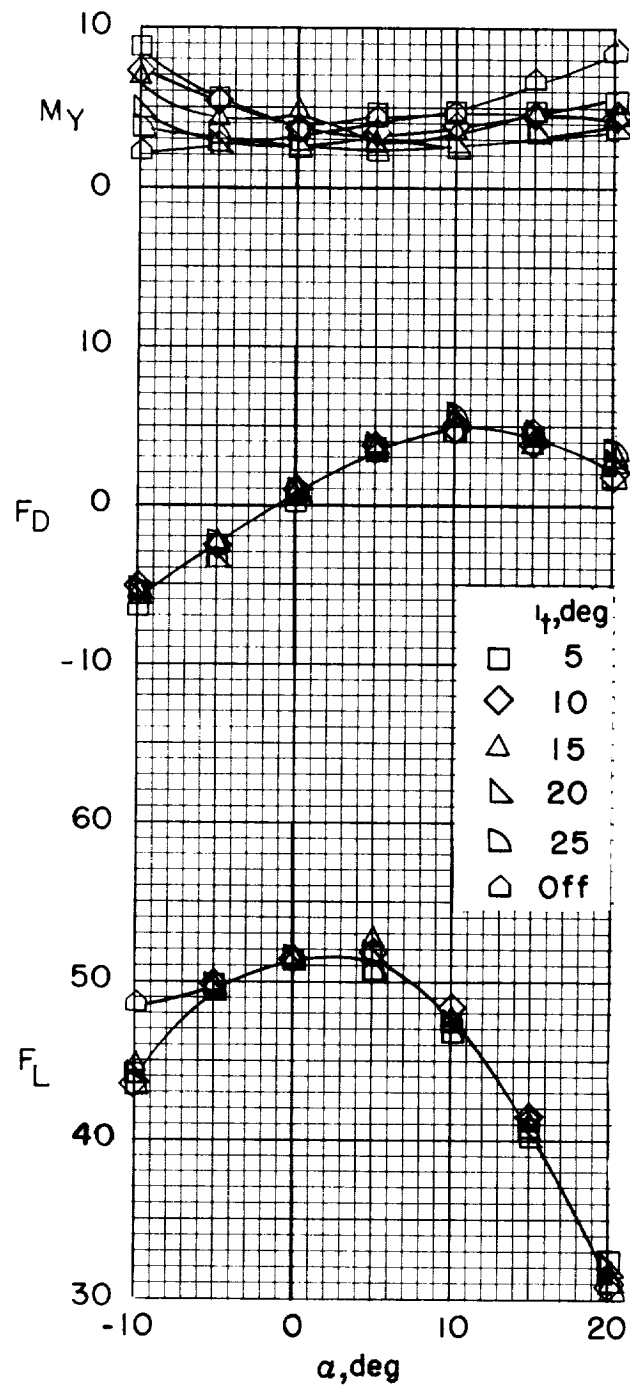
(b) $i_w = 70^\circ$; $V = 8.9$ feet per second.

Figure 5.- Continued.



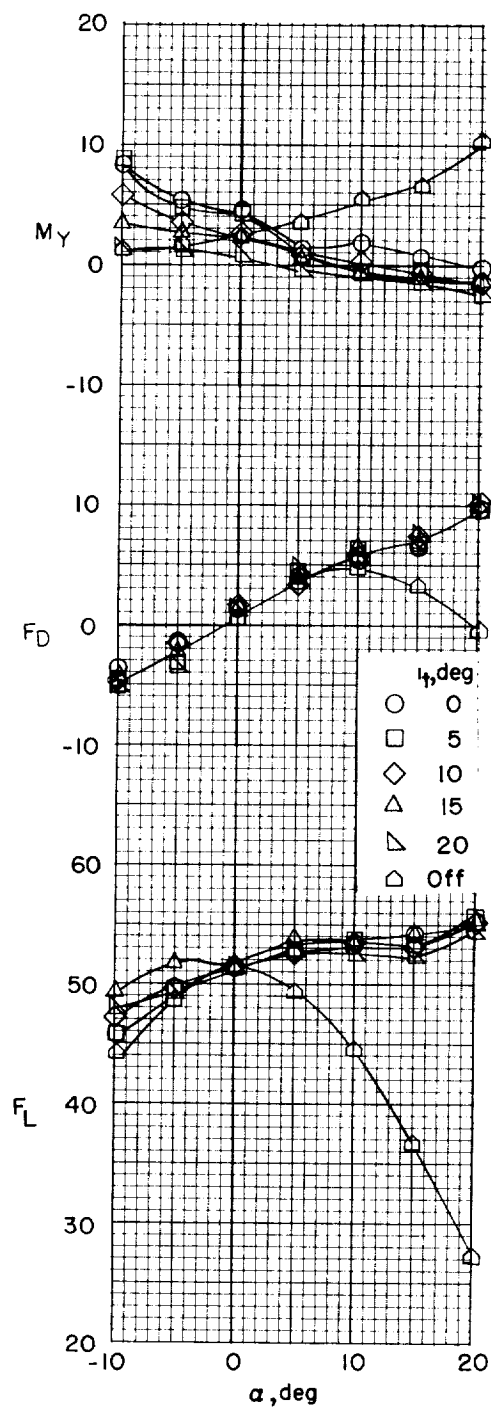
(c) $i_w = 60^\circ$; $V = 16.9$ feet per second.

Figure 5.- Continued.



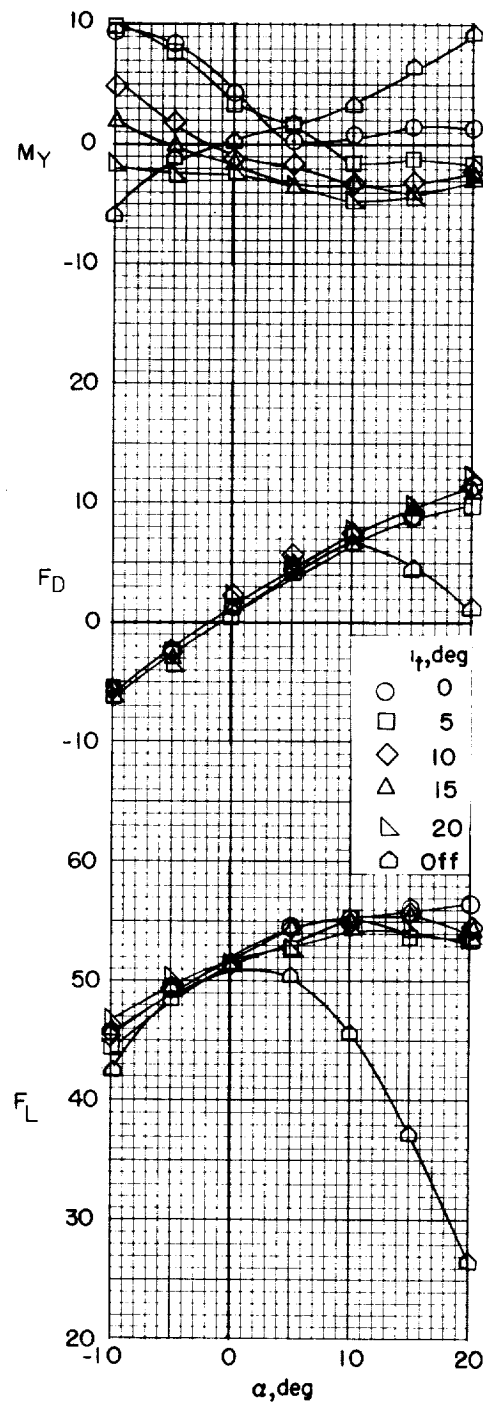
(d) $i_w = 50^\circ$; $V = 27.6$ feet per second.

Figure 5.- Continued.



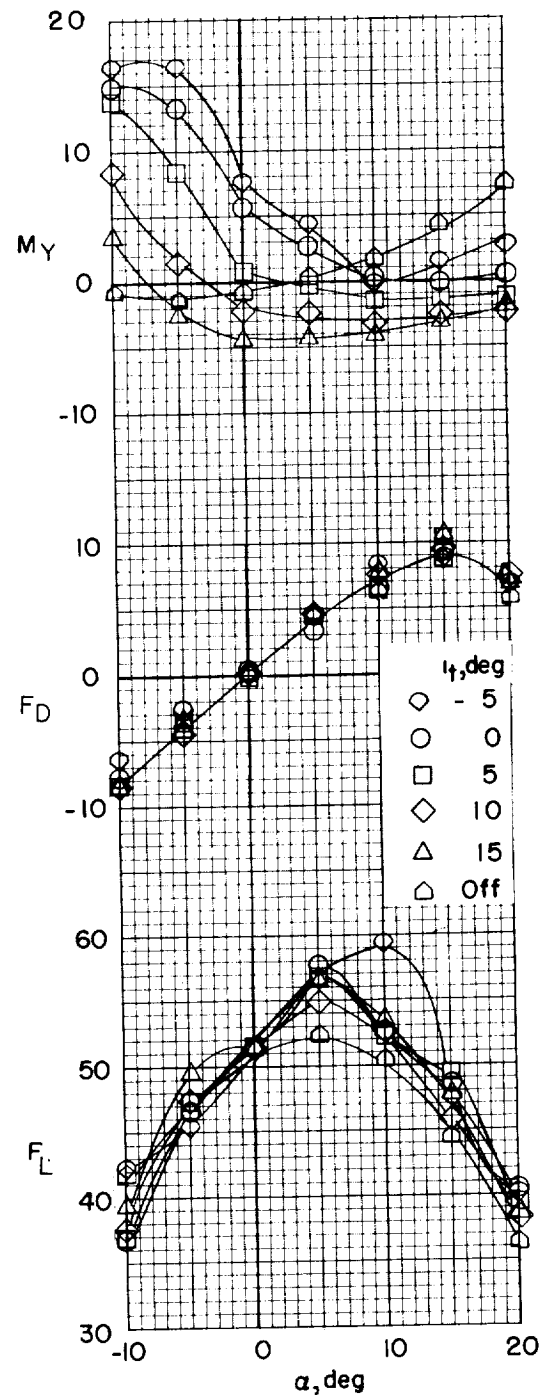
(e) $i_w = 40^\circ$; $V = 35.1$ feet per second.

Figure 5.- Continued.



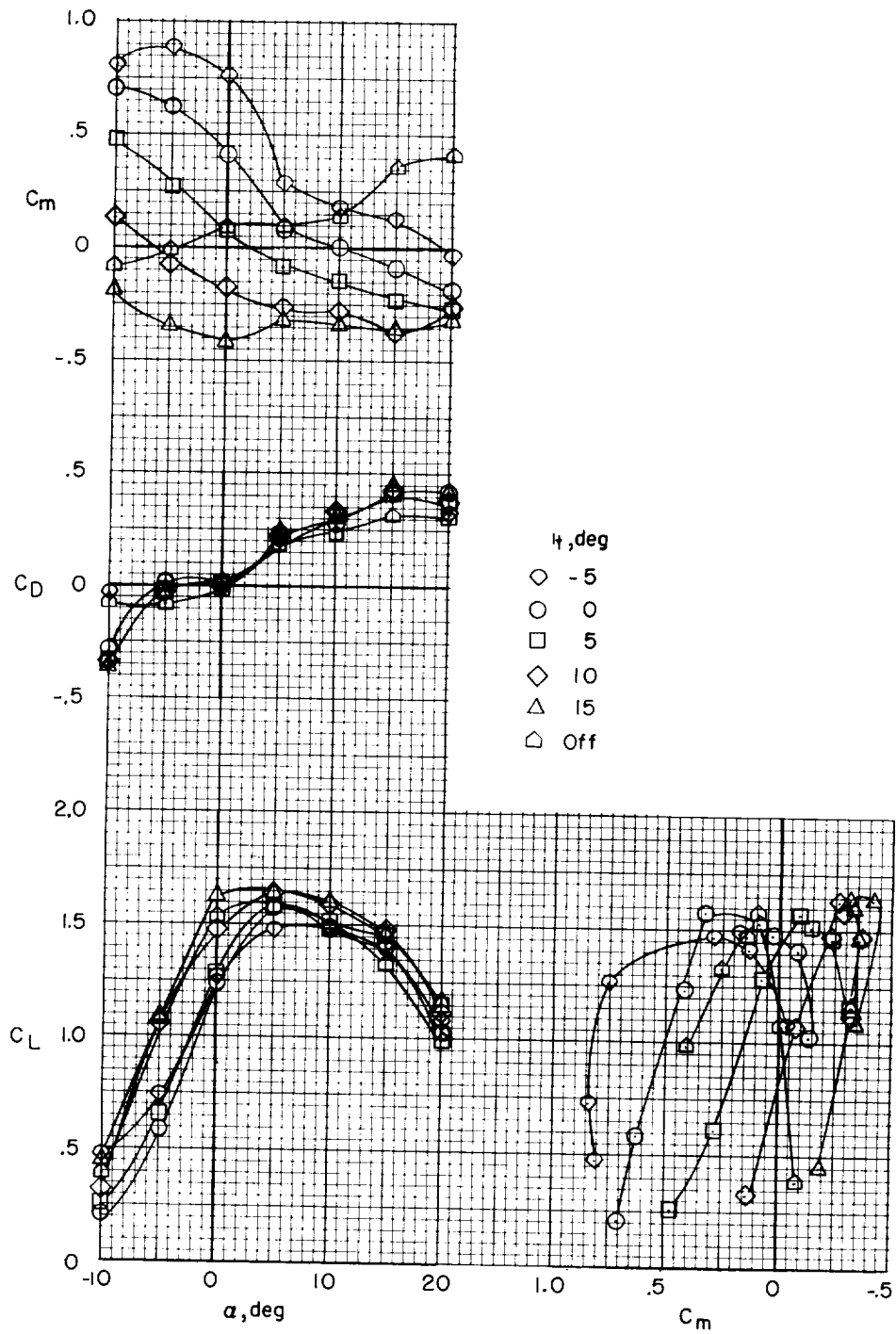
(f) $i_w = 30^\circ$; $V = 41.9$ feet per second.

Figure 5.- Continued.



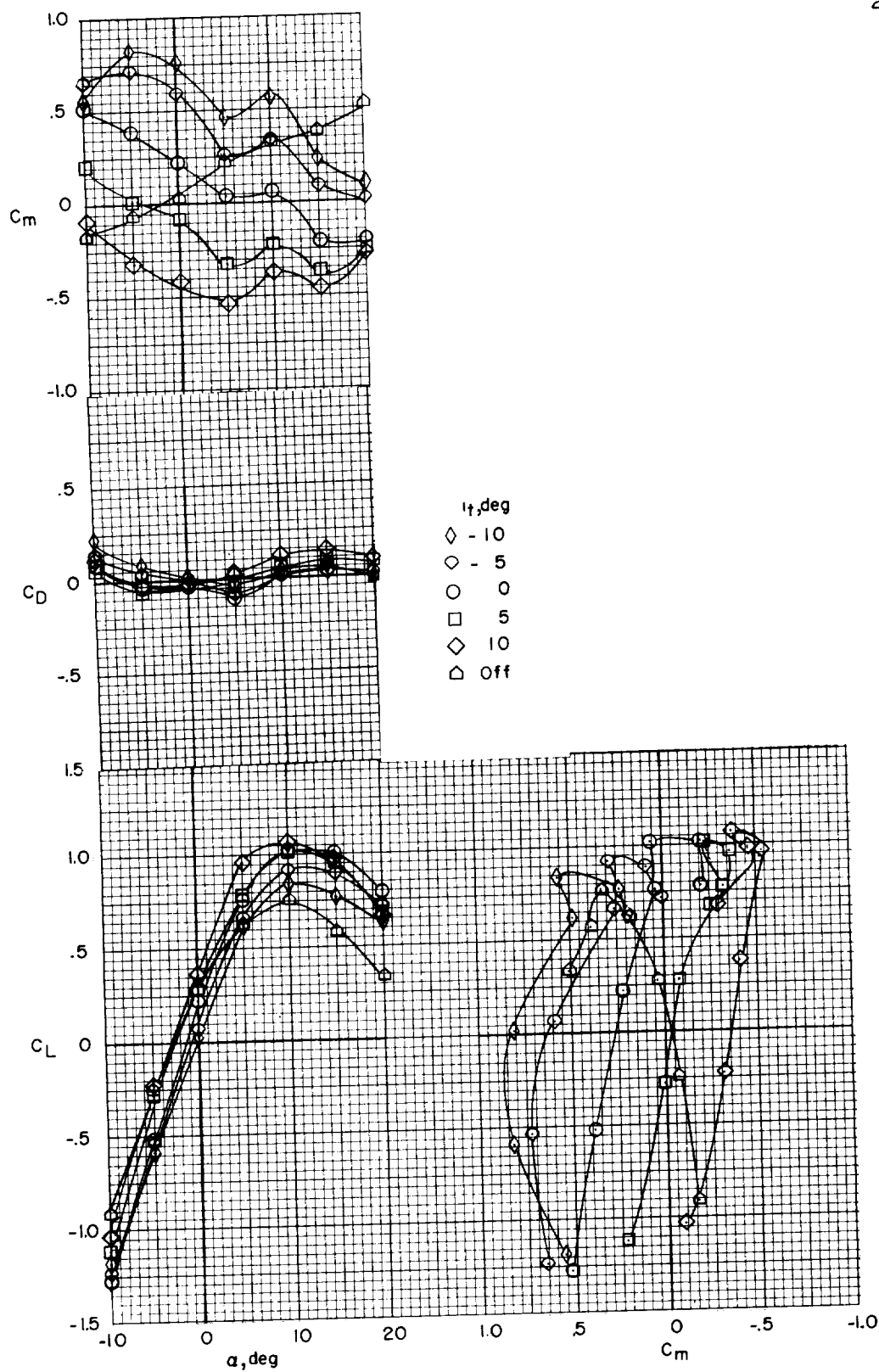
(g) $i_w = 20^\circ$; $V = 55.3$ feet per second.

Figure 5.- Continued.



(h) $i_w = 10^\circ$.

Figure 5.- Continued.



(i) $i_w = 0^\circ$.

Figure 5.- Concluded.

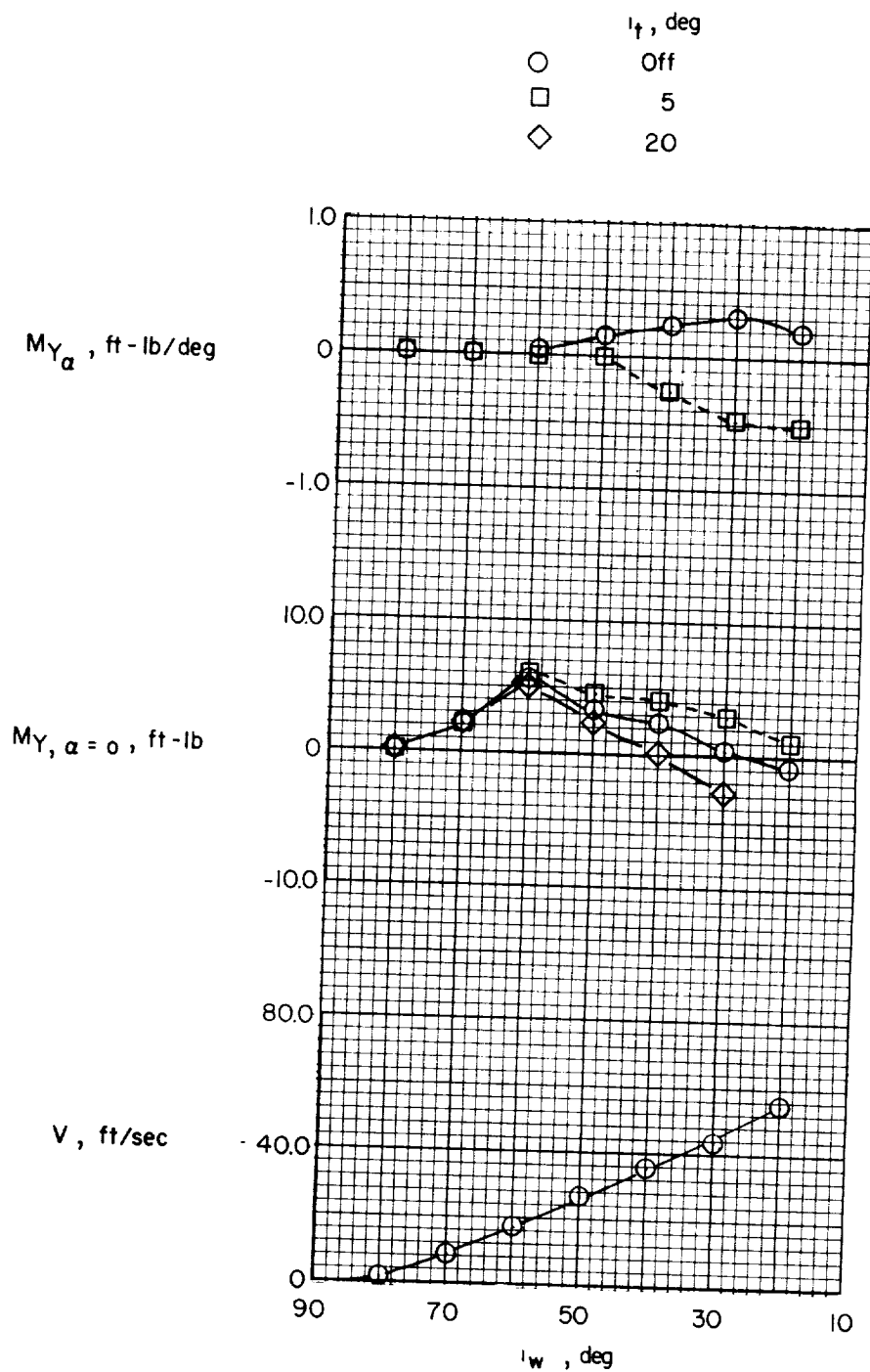
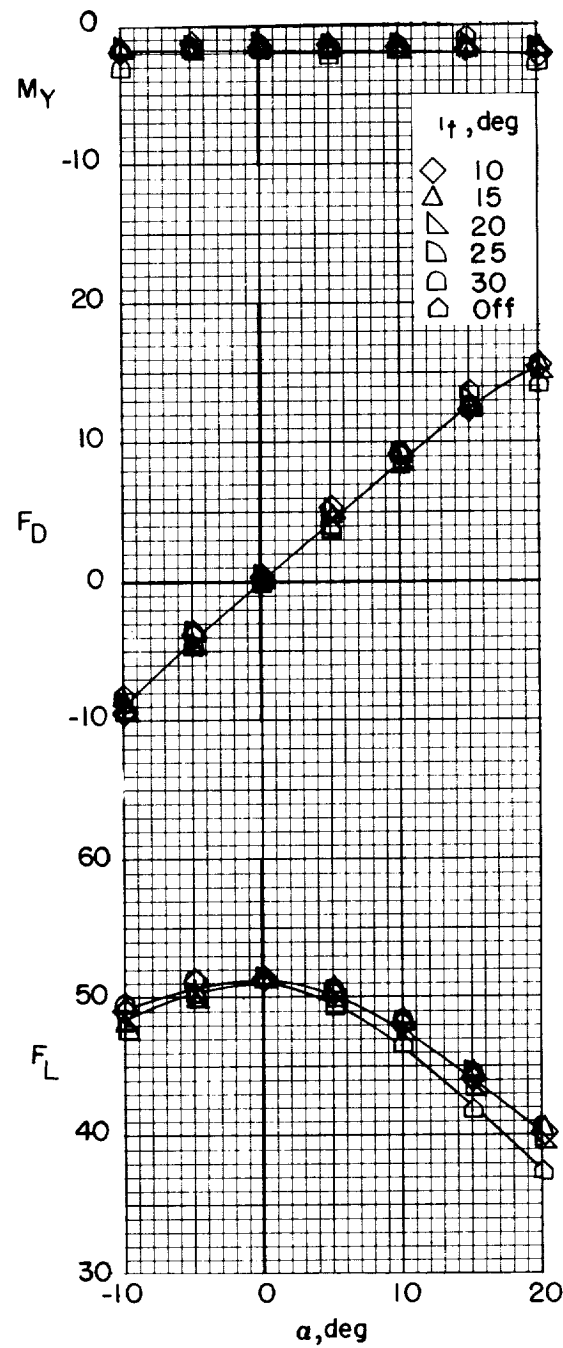
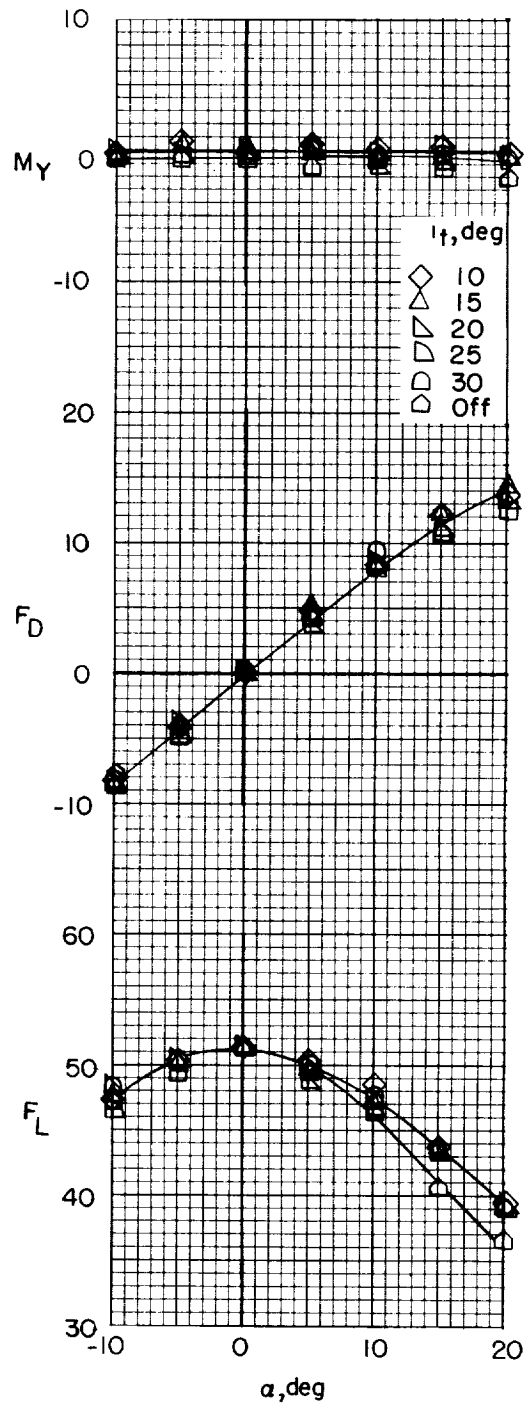


Figure 6.- Variation of longitudinal stability and trim with wing incidence for the partial-span-flap configuration with undrooped conventional aileron. Data from figure 5.



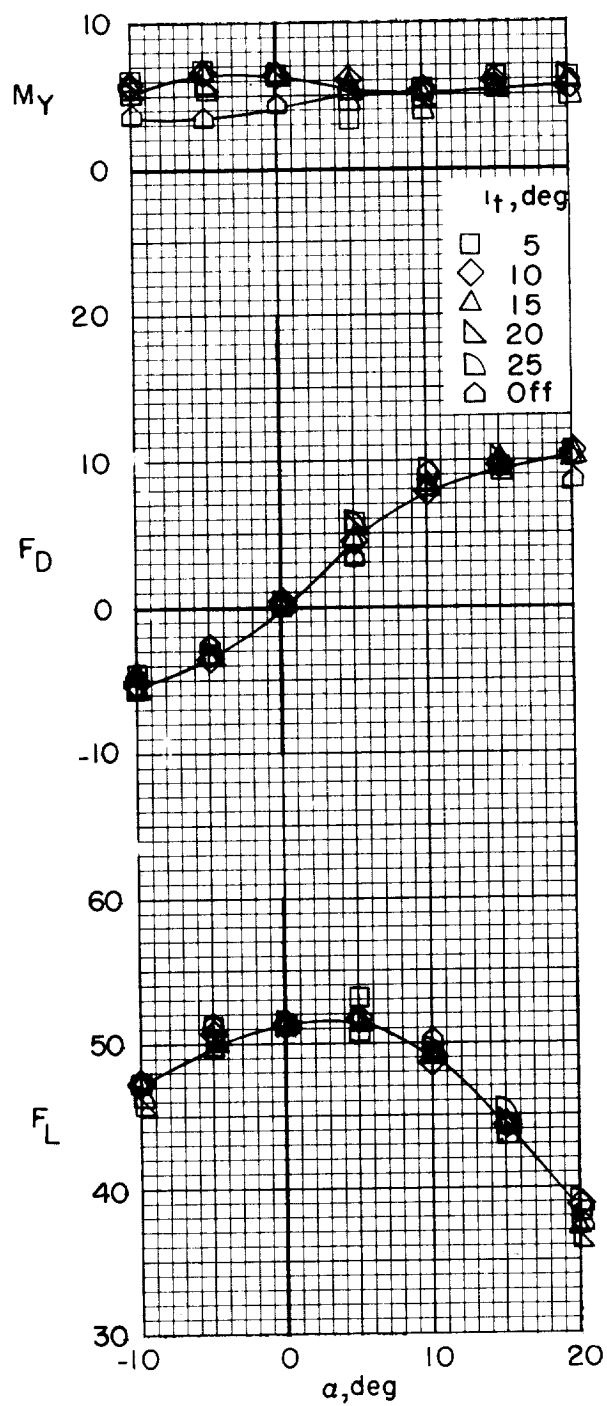
(a) $i_w = 80^\circ$; $V = 1.2$ feet per second.

Figure 7.- Longitudinal stability and control characteristics of the partial-span-flap configuration with drooped conventional aileron.



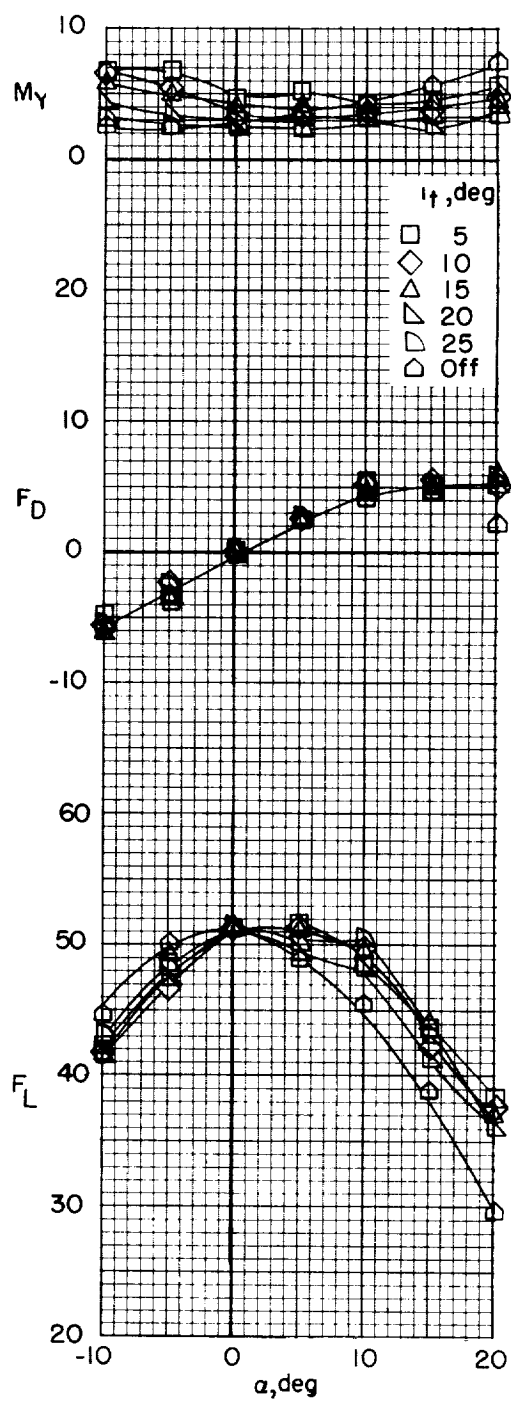
(b) $i_w = 70^\circ$; $V = 7.6$ feet per second.

Figure 7.- Continued.



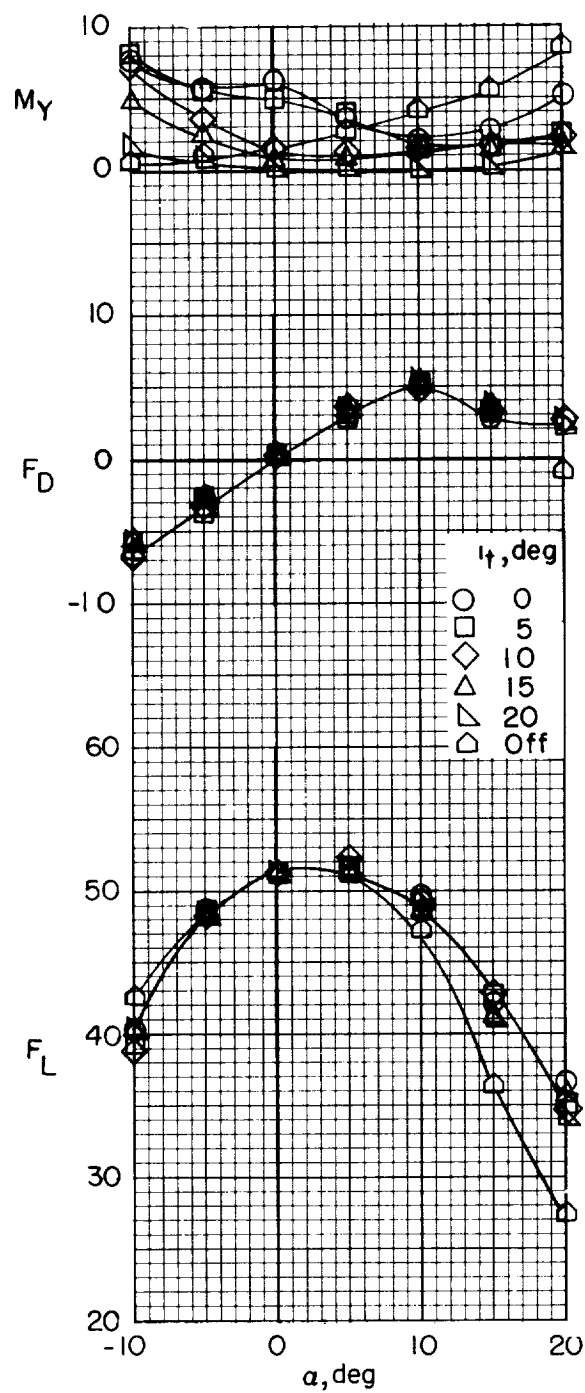
(c) $i_w = 60^\circ$; $V = 16.3$ feet per second.

Figure 7.- Continued.



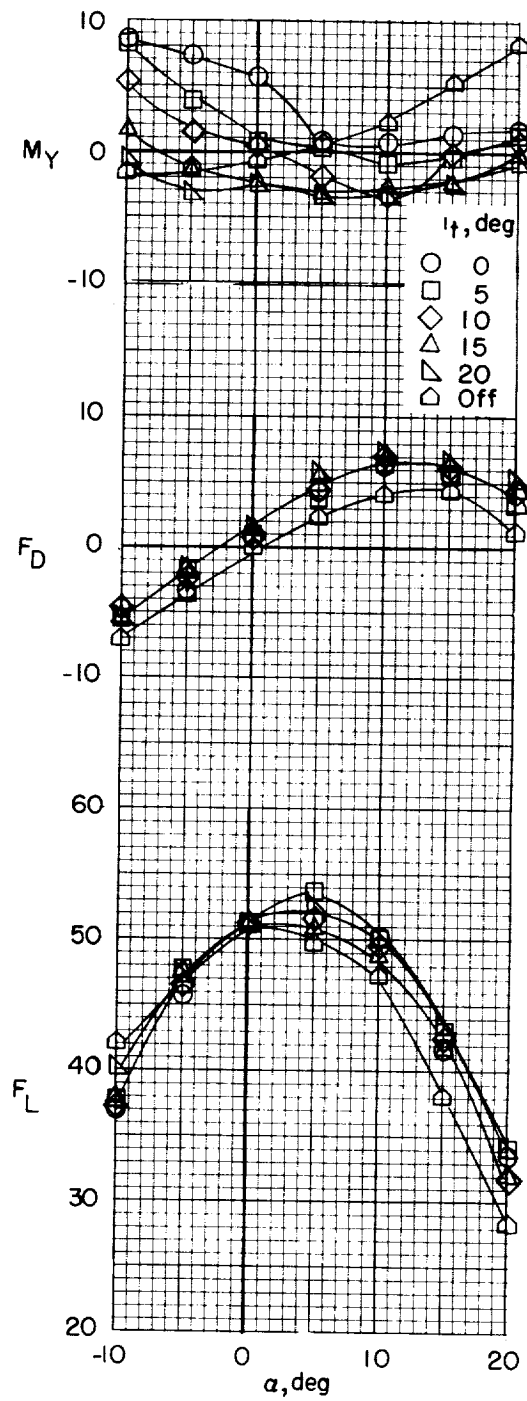
(d) $i_w = 50^\circ$; $V = 26.2$ feet per second.

Figure 7.- Continued.



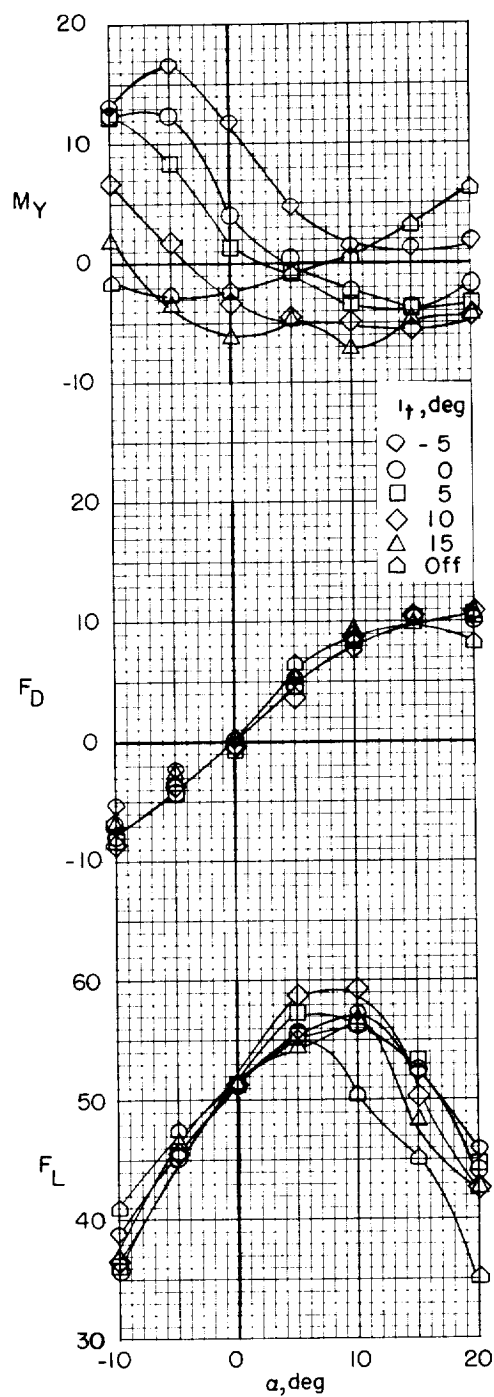
(e) $i_w = 40^\circ$; $V = 32.2$ feet per second.

Figure 7.- Continued.



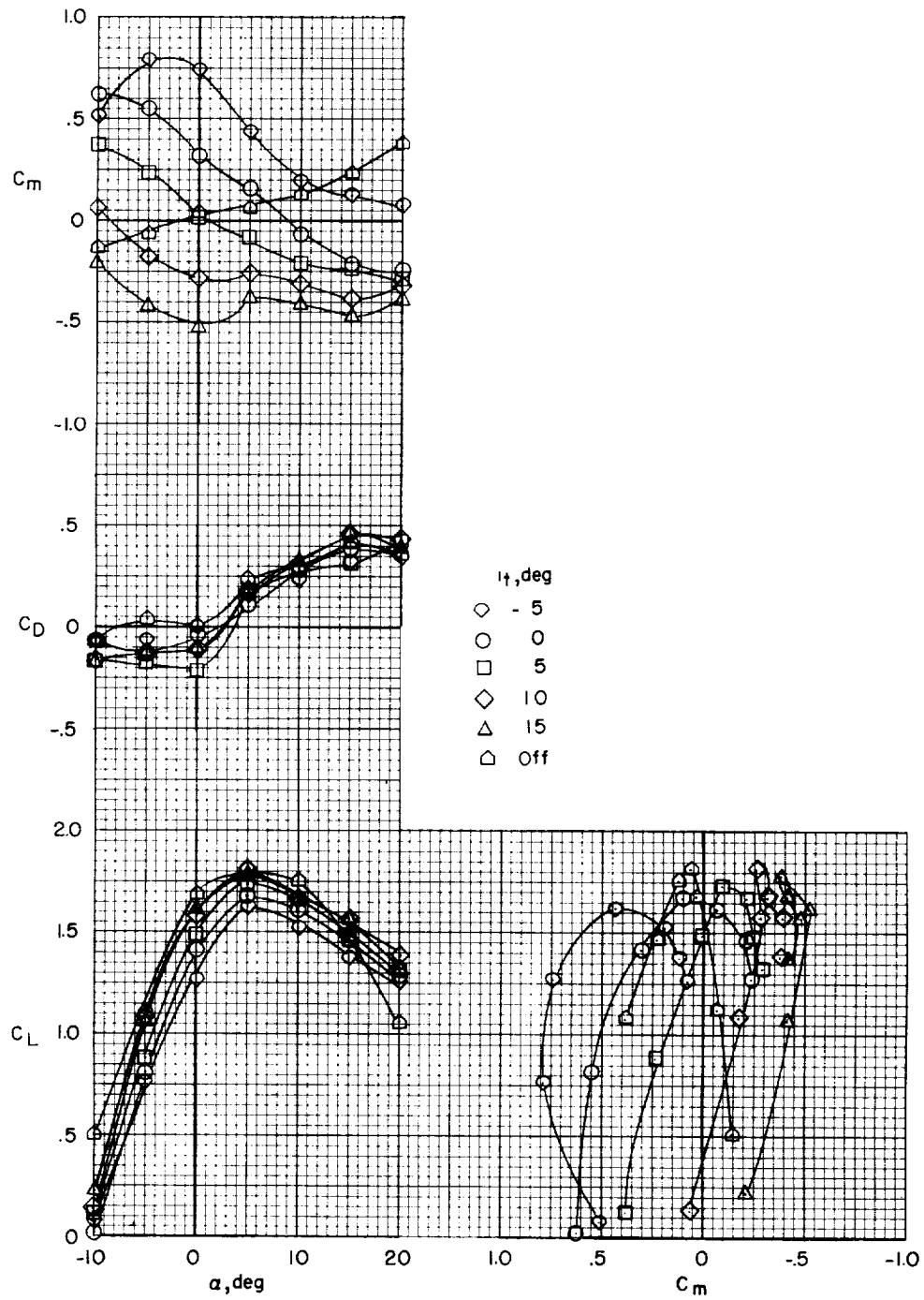
(f) $i_w = 30^\circ$; $V = 40.0$ feet per second.

Figure 7.- Continued.



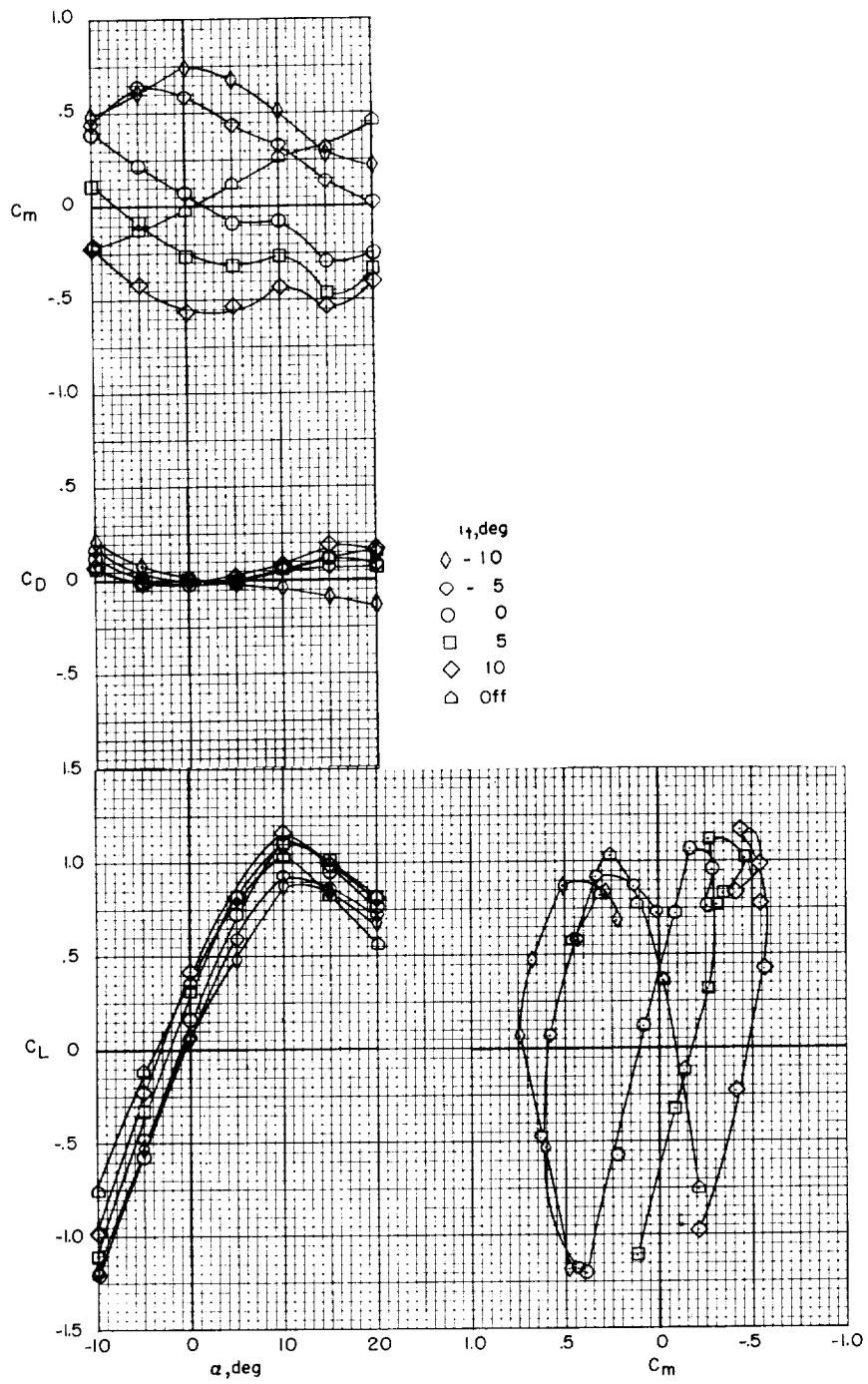
(g) $I_w = 20^\circ$; $V = 54.4$ feet per second.

Figure 7.- Continued.



(h) $i_w = 10^\circ$.

Figure 7.- Continued.



(i) $i_w = 0^\circ$.

Figure 7.- Concluded.

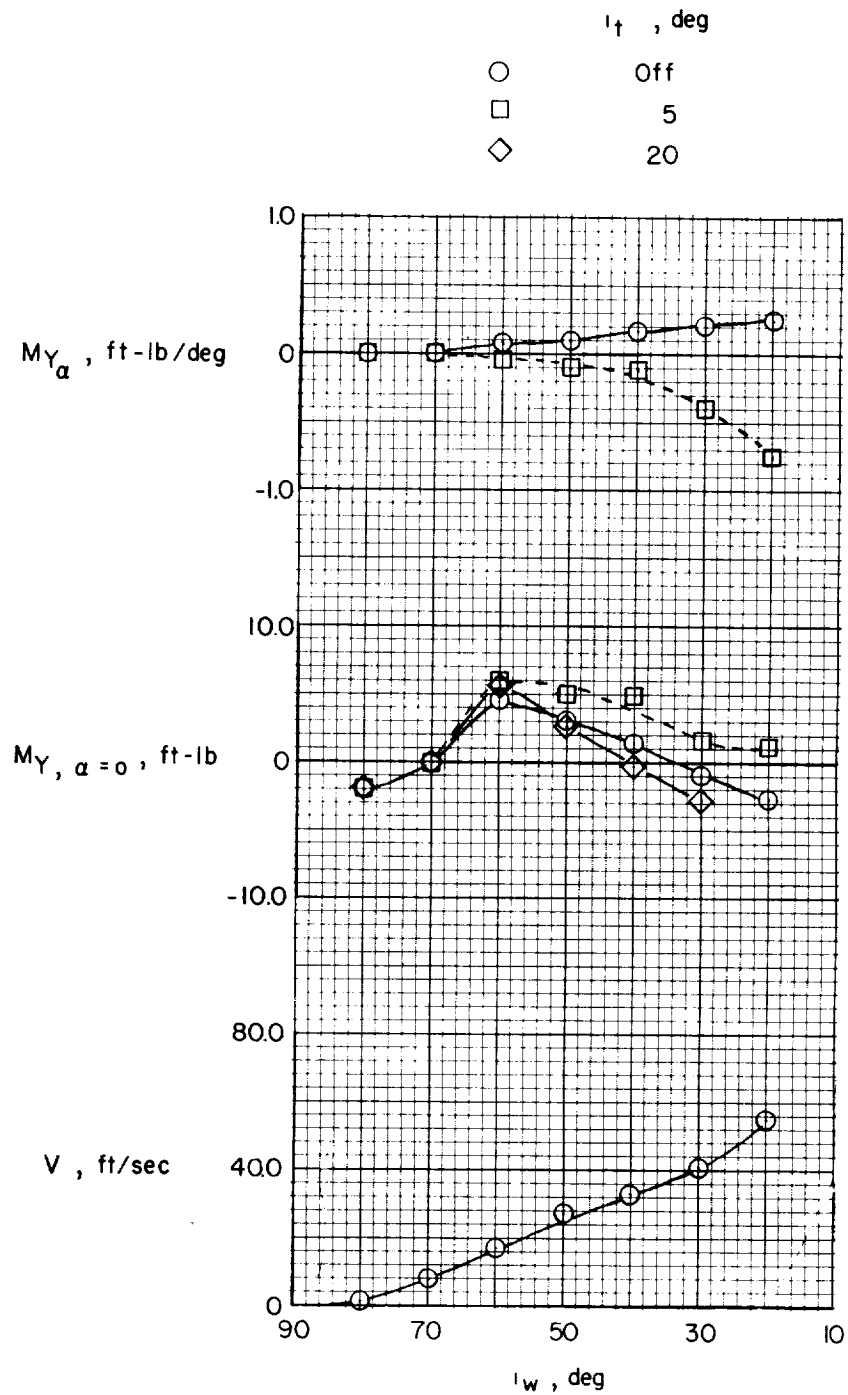
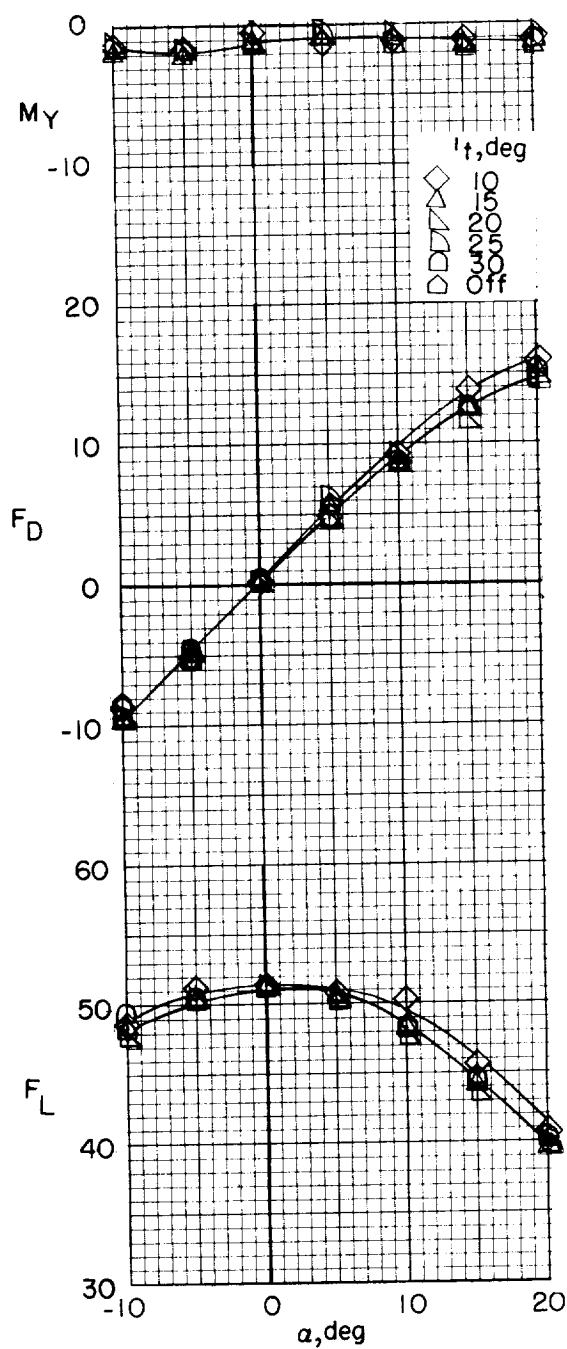
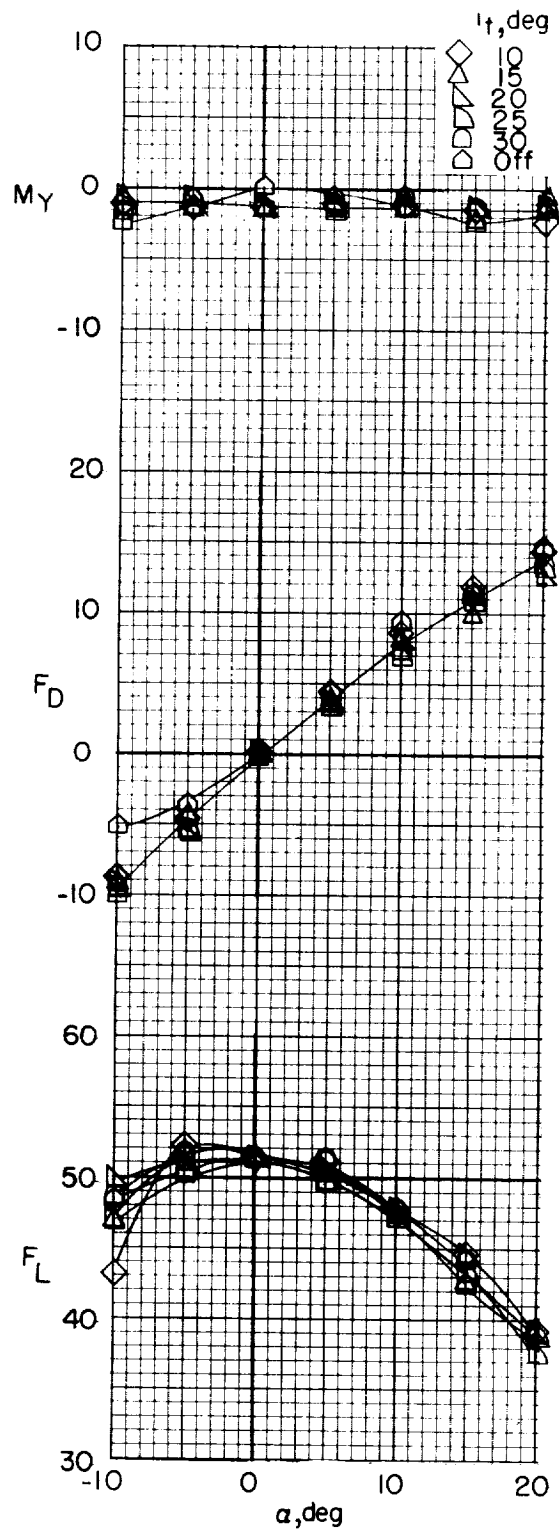


Figure 8.- Variation of longitudinal stability and trim with wing incidence for the partial-span-flap configuration with drooped conventional aileron. Data from figure 7.



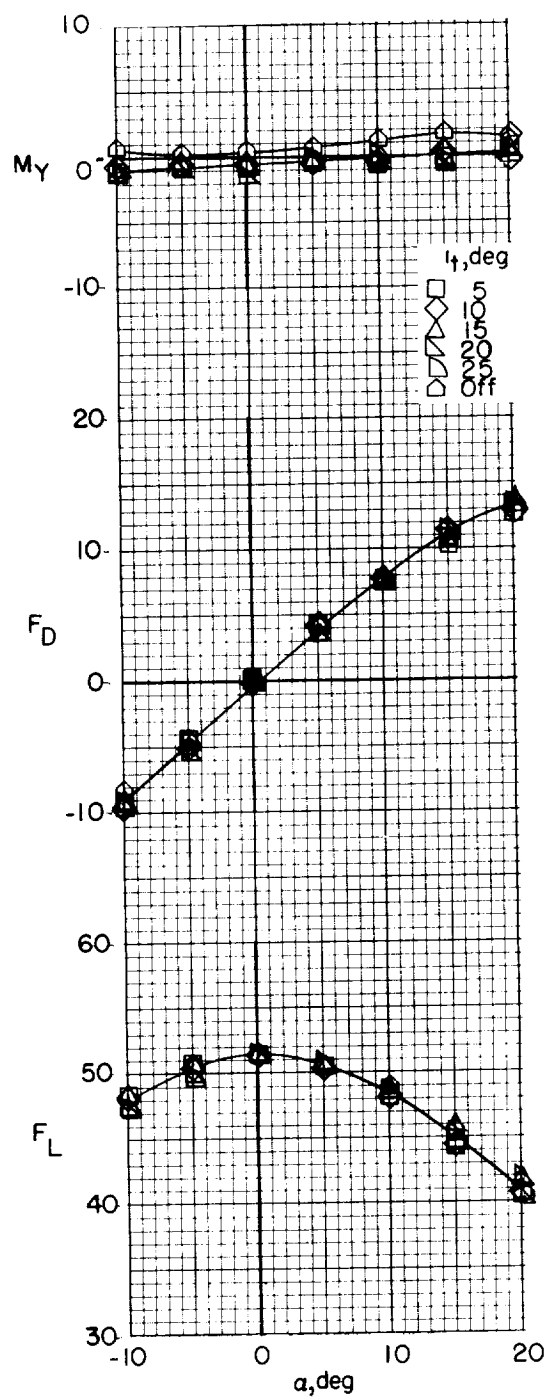
(a) $i_w = 80^\circ$; $V = 1.2$ feet per second.

Figure 9.- Longitudinal stability and control characteristics of the full-span-flap configuration with slot-lip aileron.



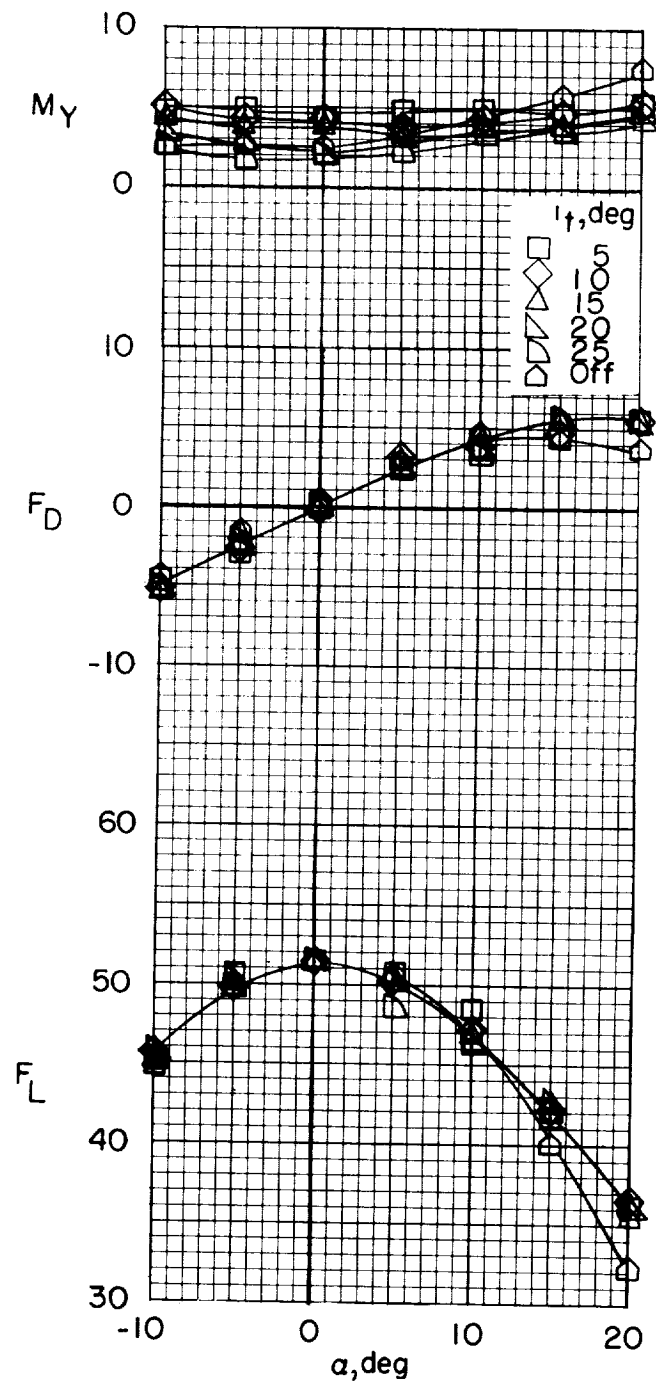
(b) $I_w = 70^\circ$; $V = 7.8$ feet per second.

Figure 9.- Continued.



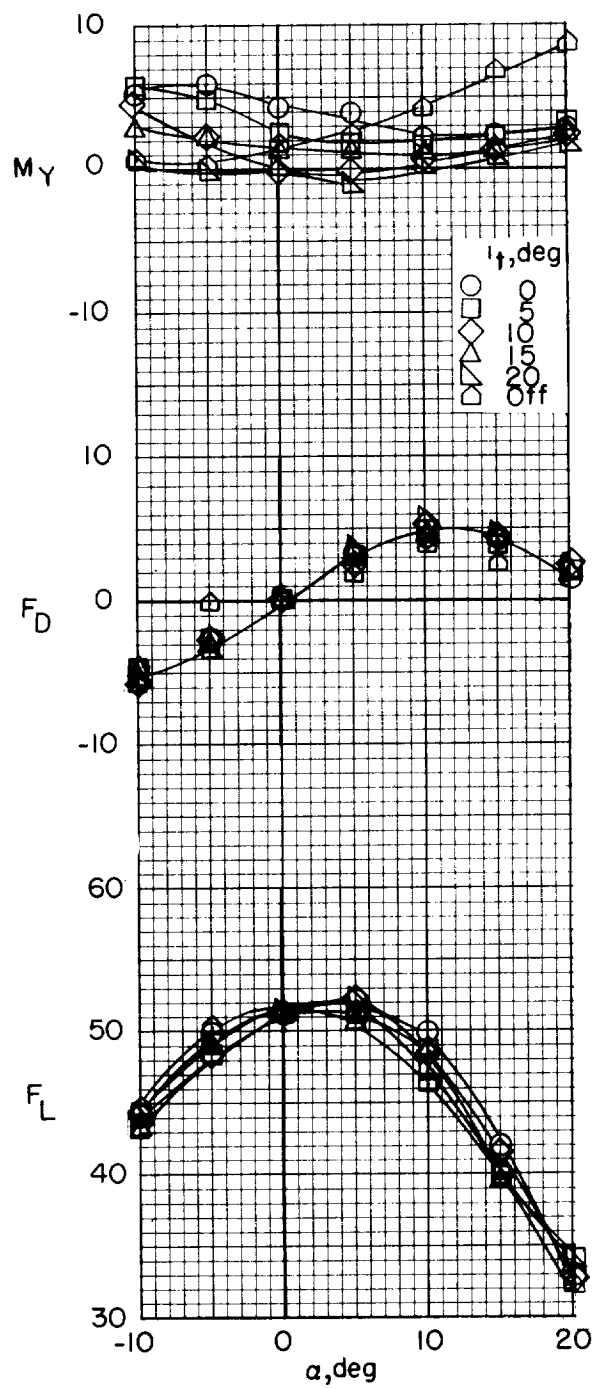
(c) $i_w = 60^\circ$; $V = 11.8$ feet per second.

Figure 9.- Continued.



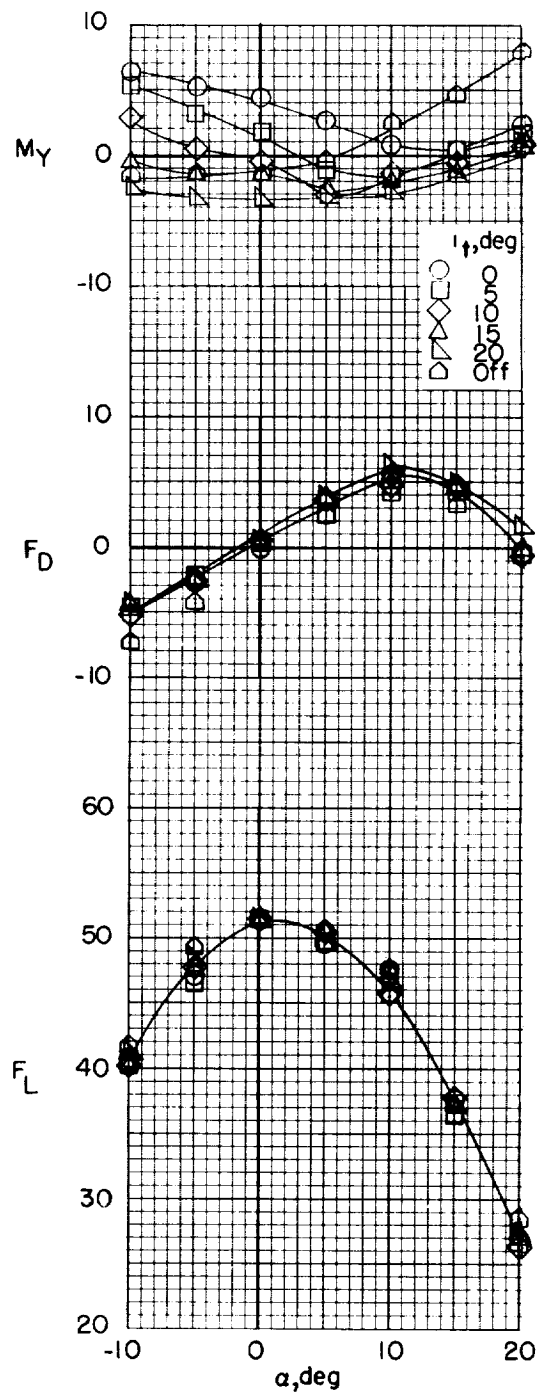
(d) $i_w = 50^\circ$; $V = 23.8$ feet per second.

Figure 9.- Continued.



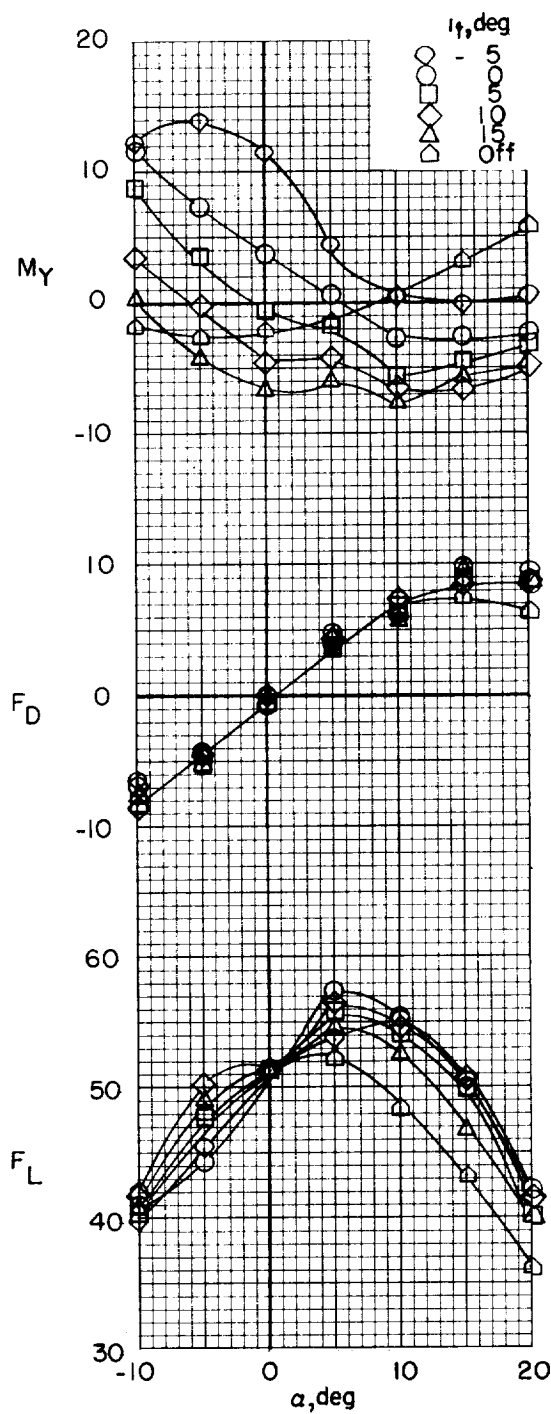
(e) $i_w = 40^\circ$; $V = 31.2$ feet per second.

Figure 9.- Continued.



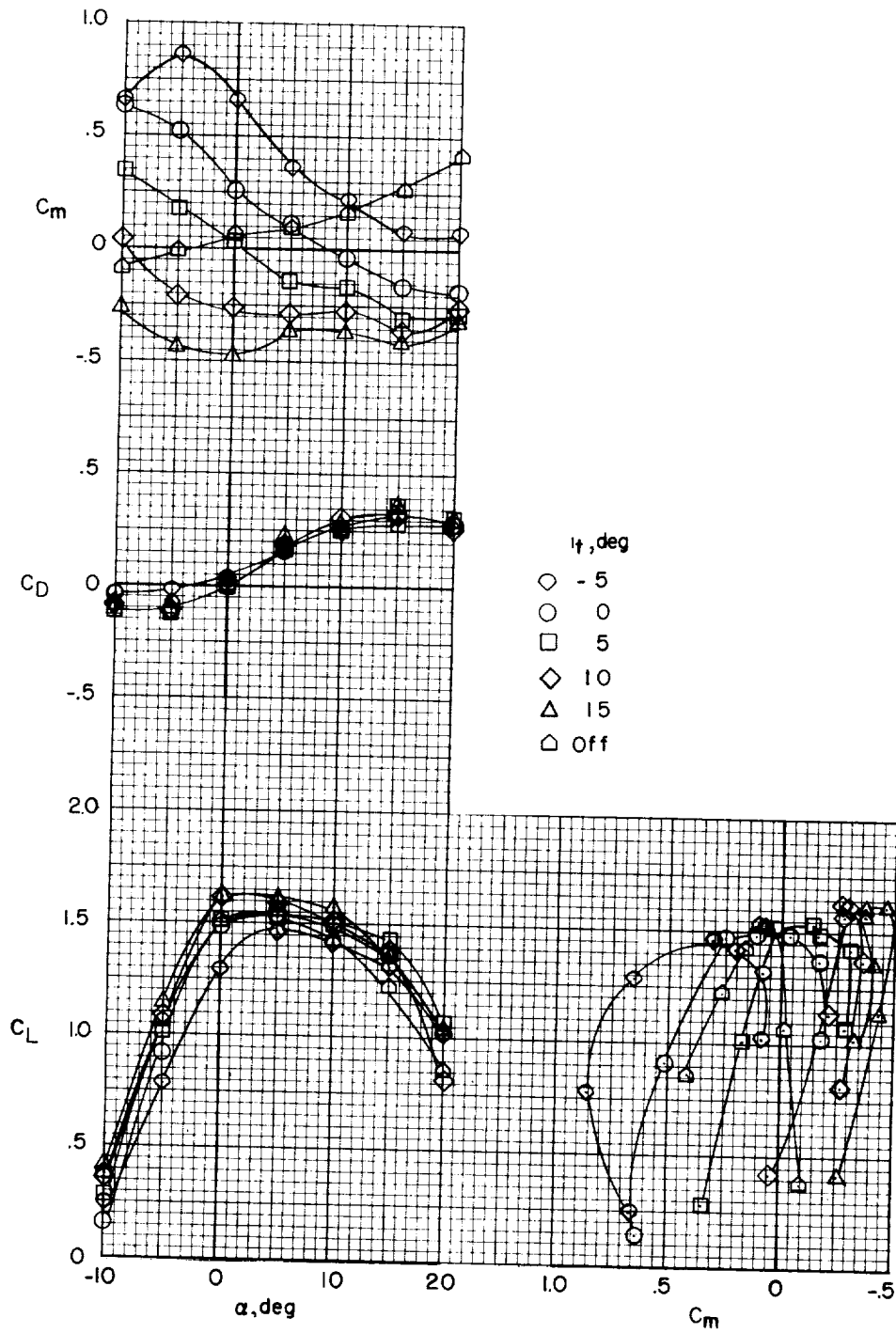
(f) $i_w = 30^\circ$; $V = 40.3$ feet per second.

Figure 9.- Continued.



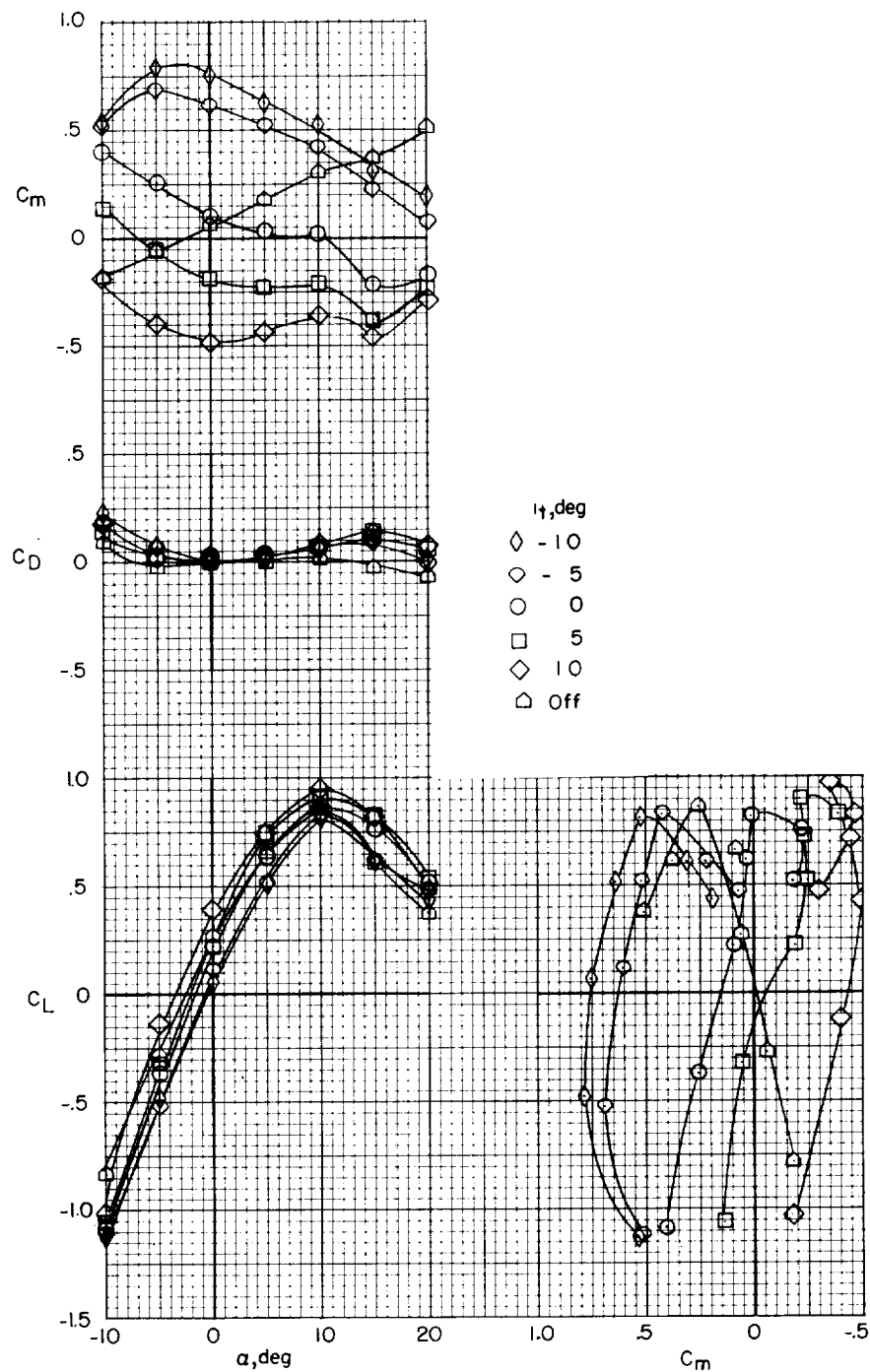
(g) $i_w = 20^\circ$; $V = 52.6$ feet per second.

Figure 9.- Continued.



(h) $i_w = 10^\circ$.

Figure 9.- Continued.



(1) $i_w = 0^\circ$.

Figure 9.- Concluded.

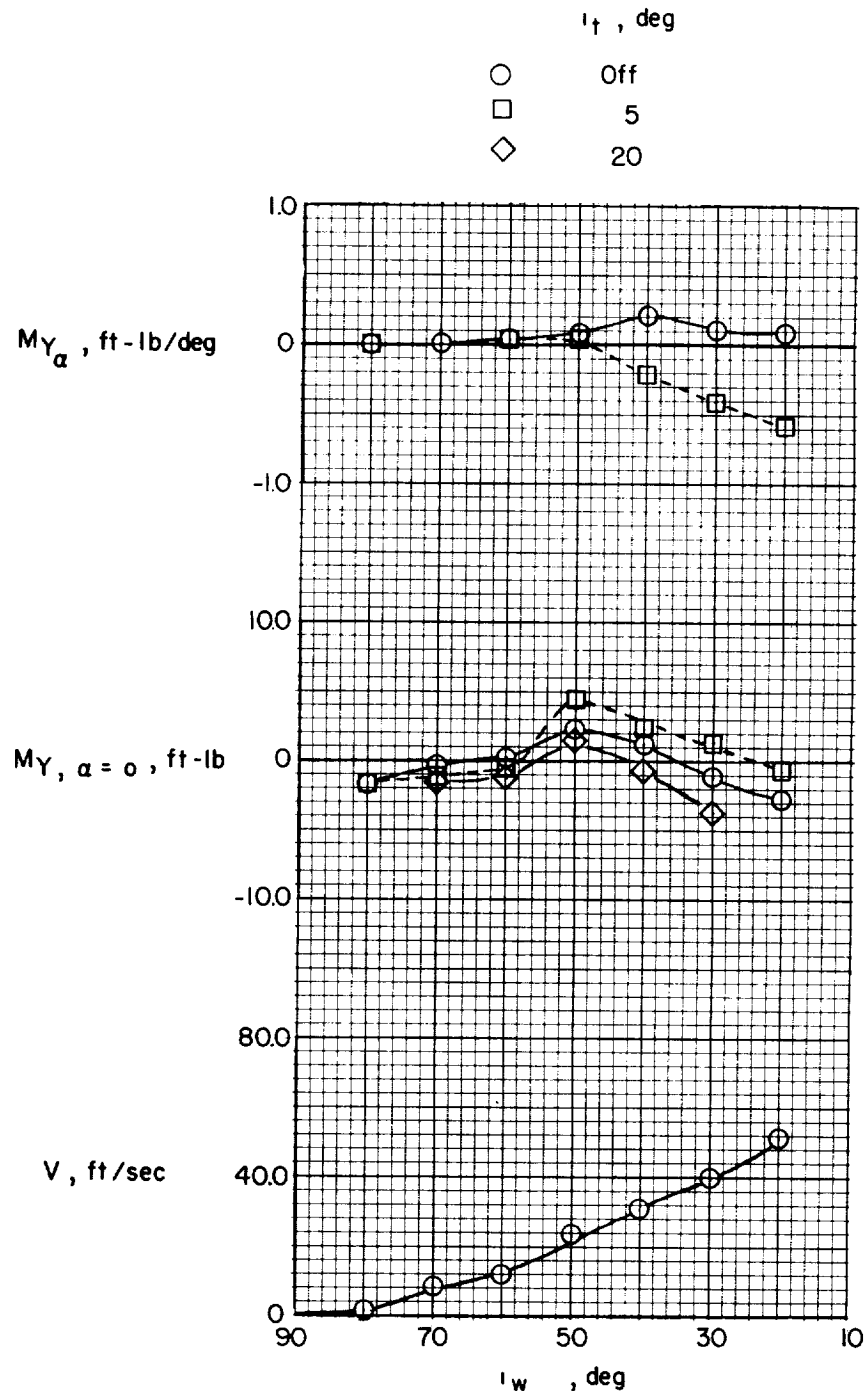
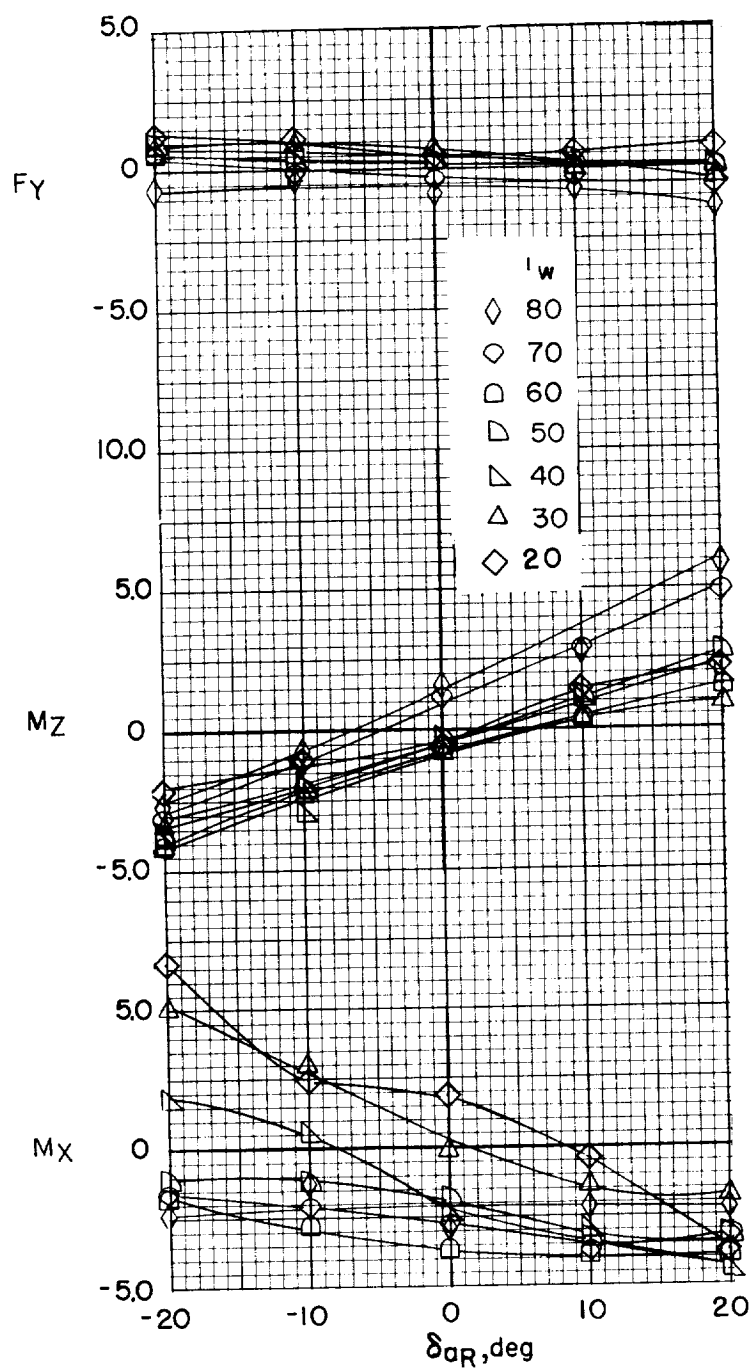
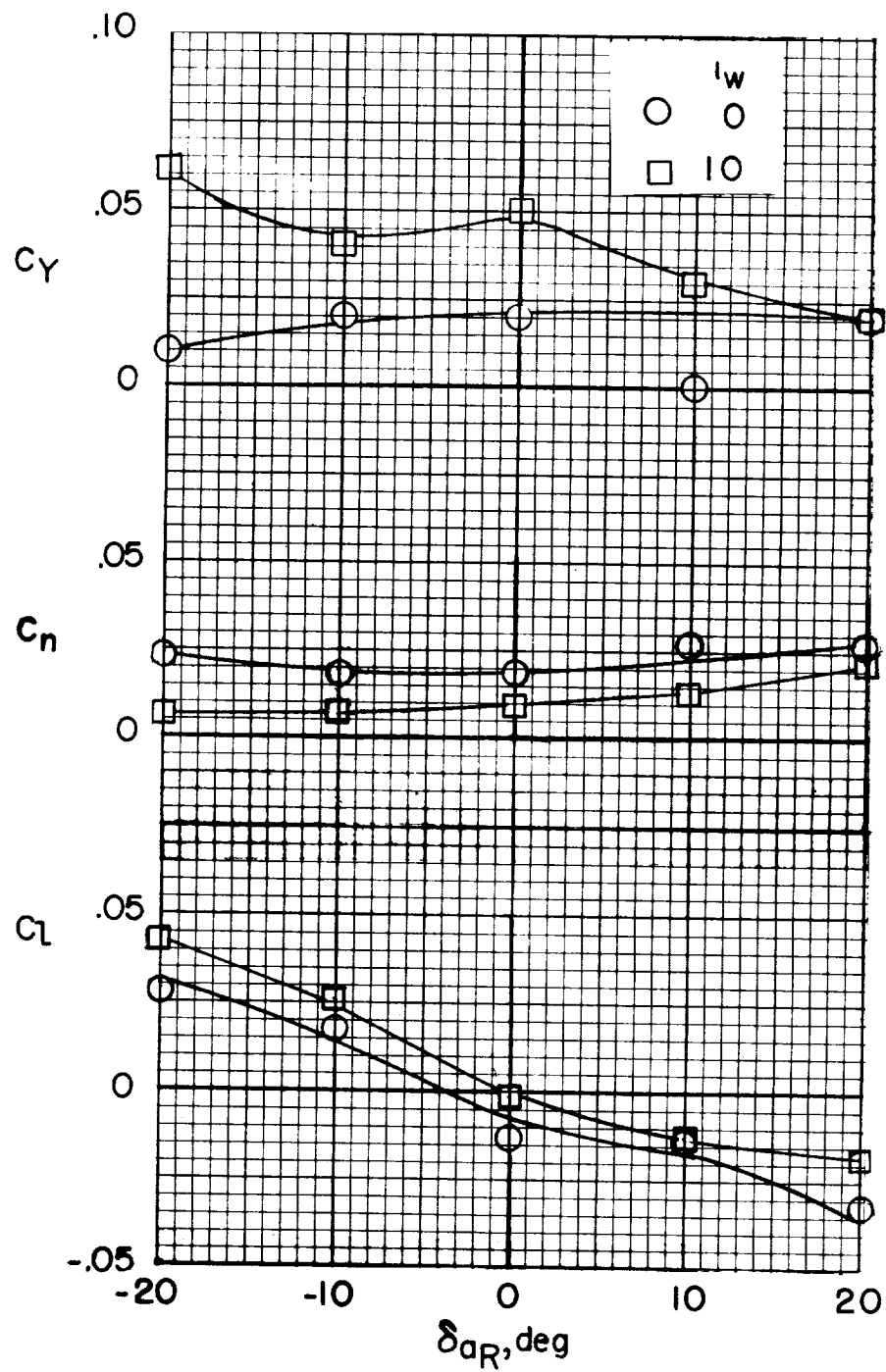


Figure 10.- Variation of longitudinal stability and trim with wing incidence for the full-span-flap configuration with slot-lip aileron. Data from figure 9.



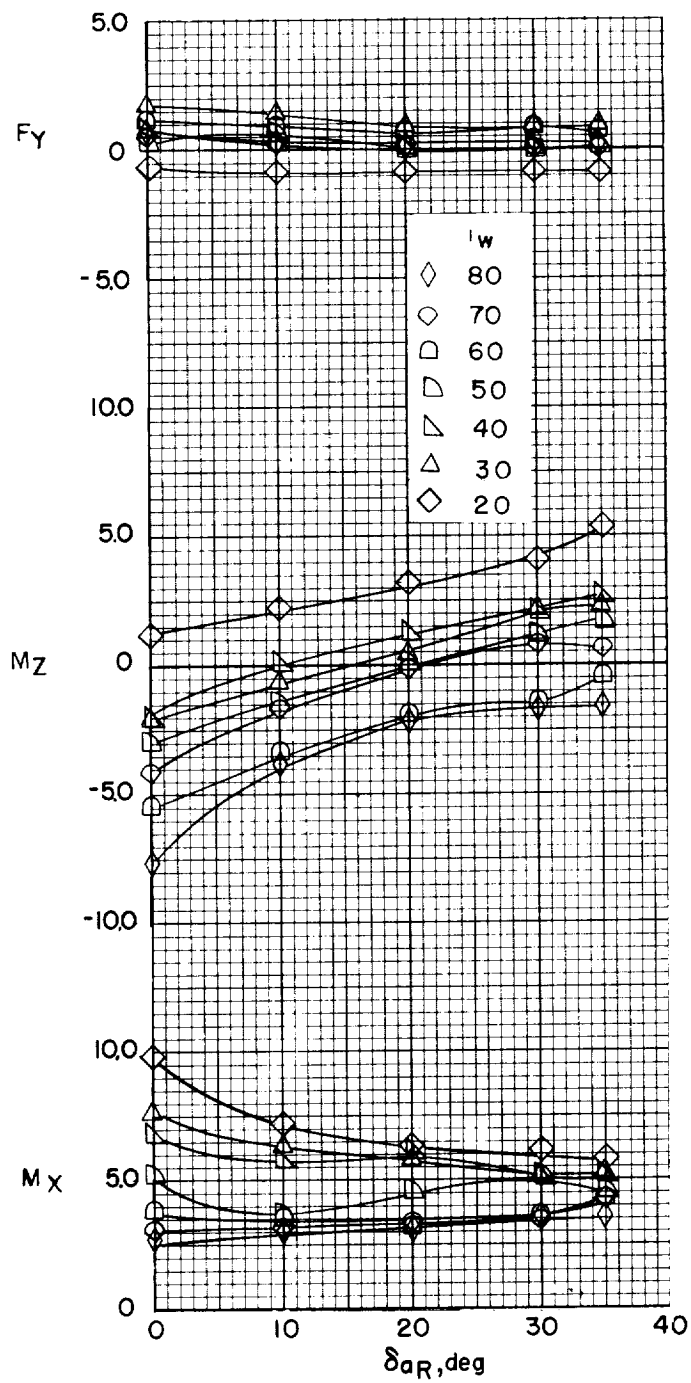
(a) Transition range.

Figure 11.- Aileron effectiveness. Partial-span flap; undrooped conventional ailerons.



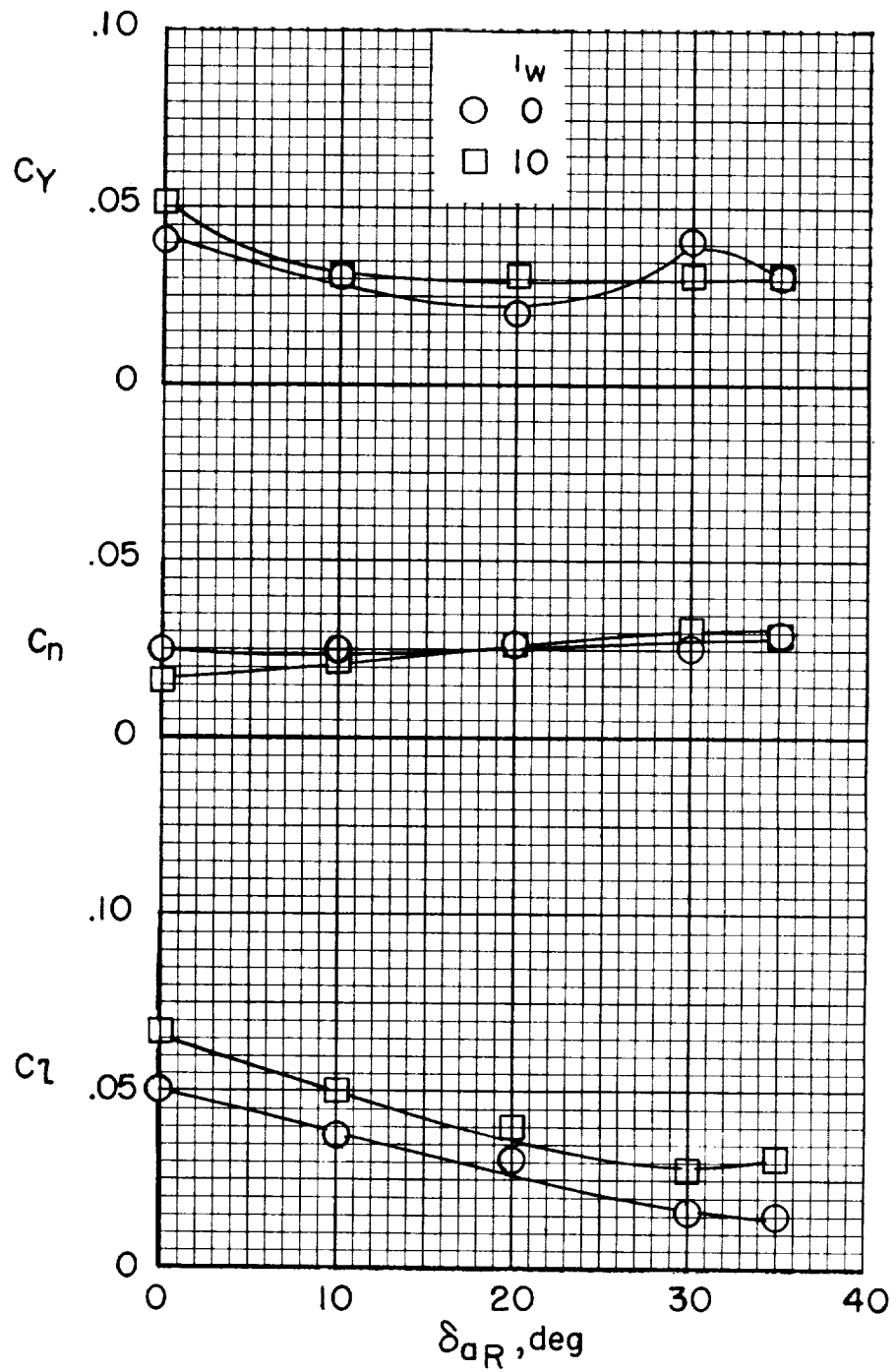
(b) Normal forward flight.

Figure 11.- Concluded.



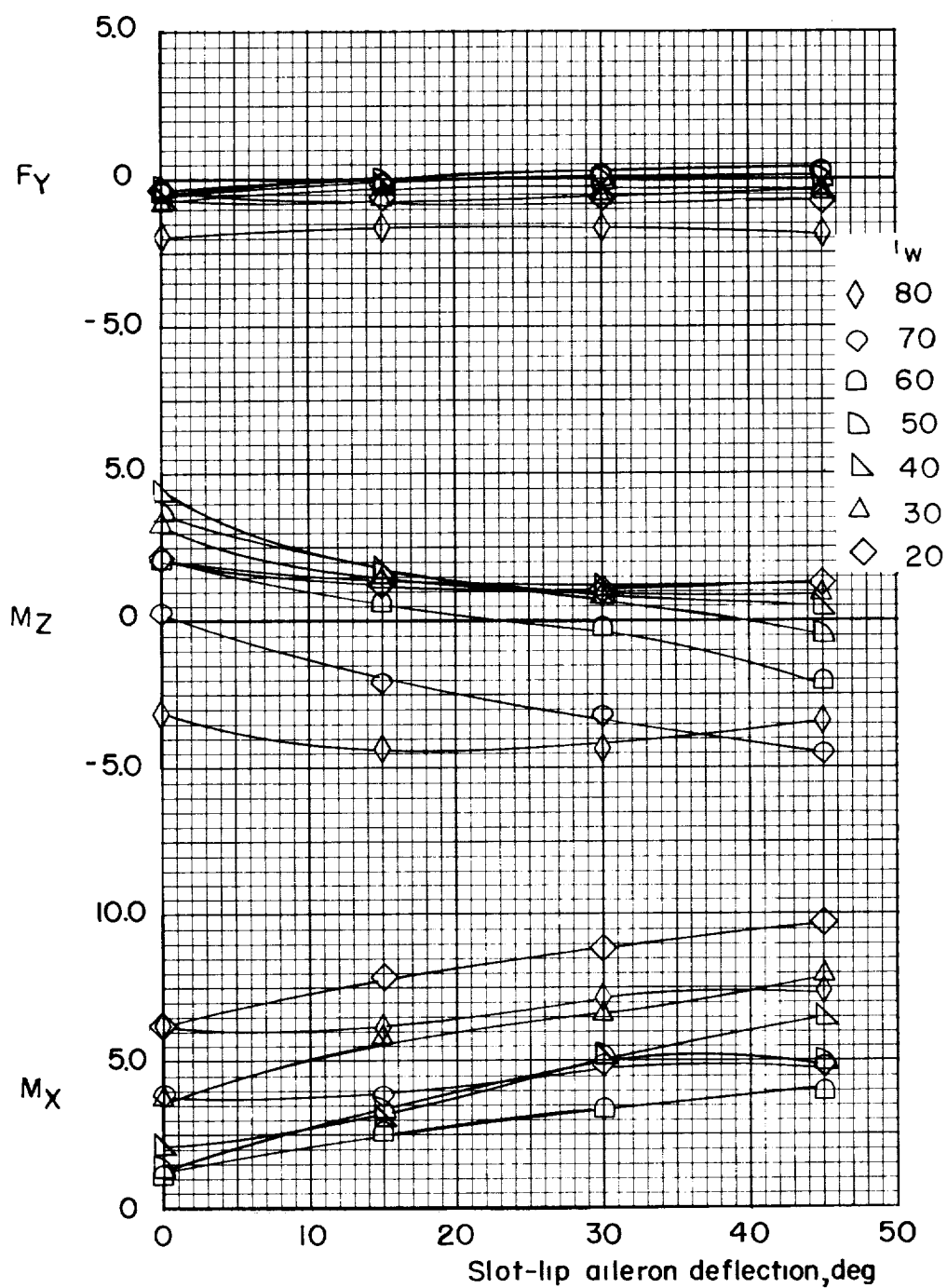
(a) Transition range.

Figure 12.- Aileron effectiveness. Partial-span flap; drooped conventional ailerons.



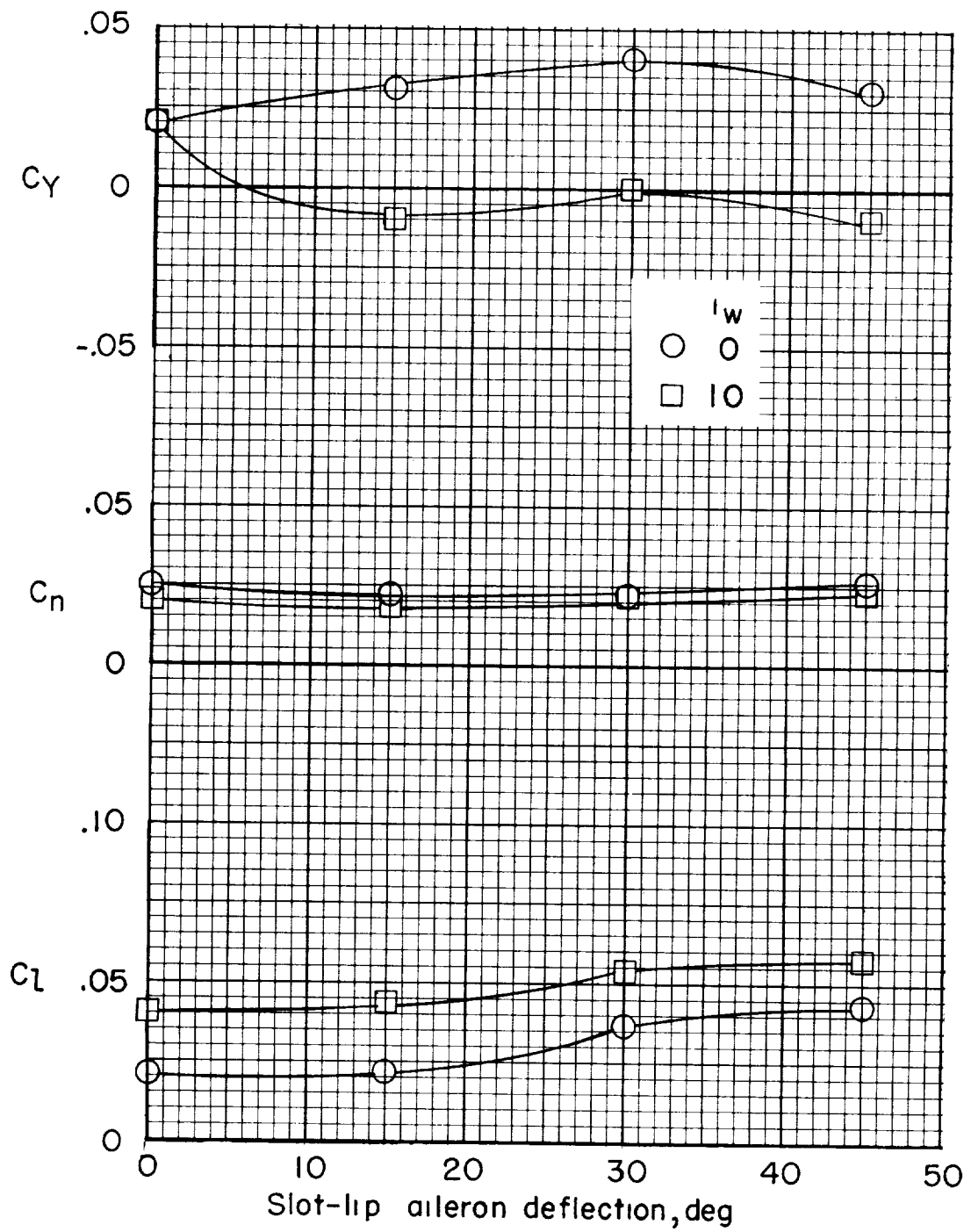
(b) Normal forward flight.

Figure 12.- Concluded.



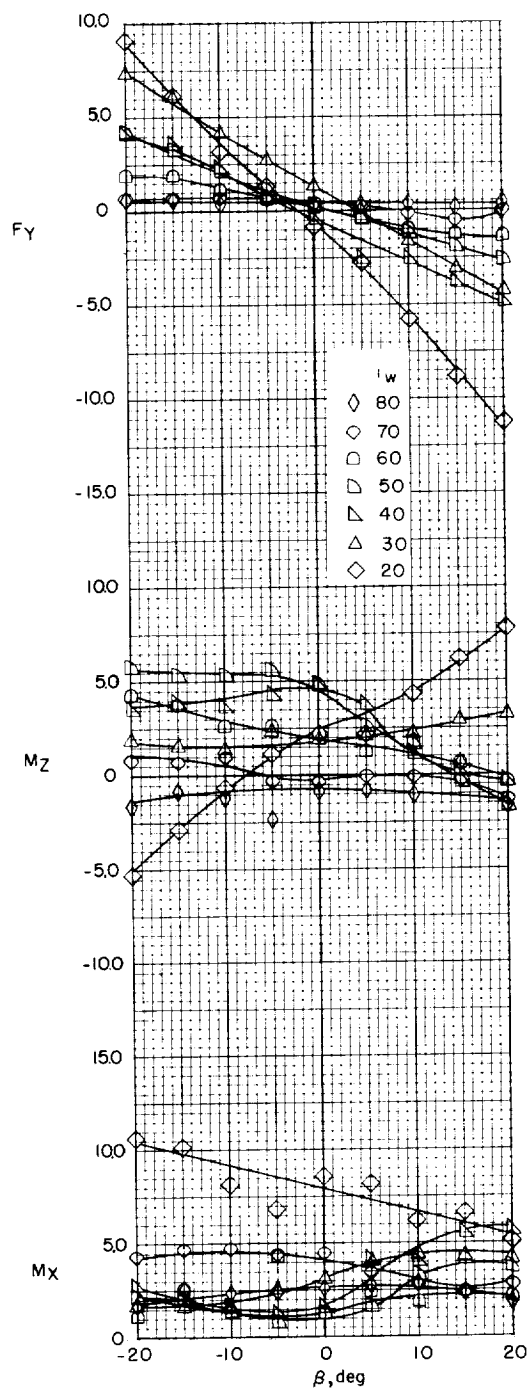
(a) Transition range.

Figure 13.- Effectiveness of the slot-lip aileron used with the full-span flap.



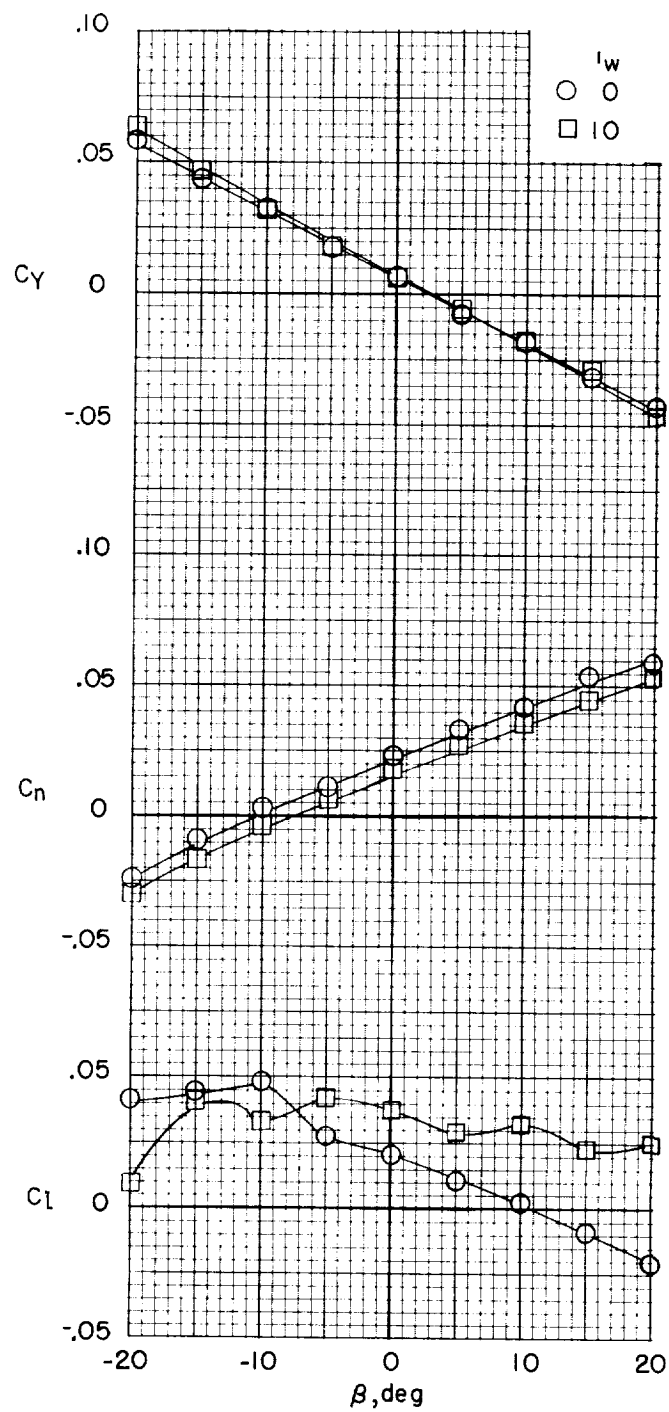
(b) Normal forward flight.

Figure 13.- Concluded.



(a) Transition range.

Figure 14.- Lateral stability characteristics of the model. Full-span-flap configuration.



(b) Normal forward flight.

Figure 14.- Concluded.

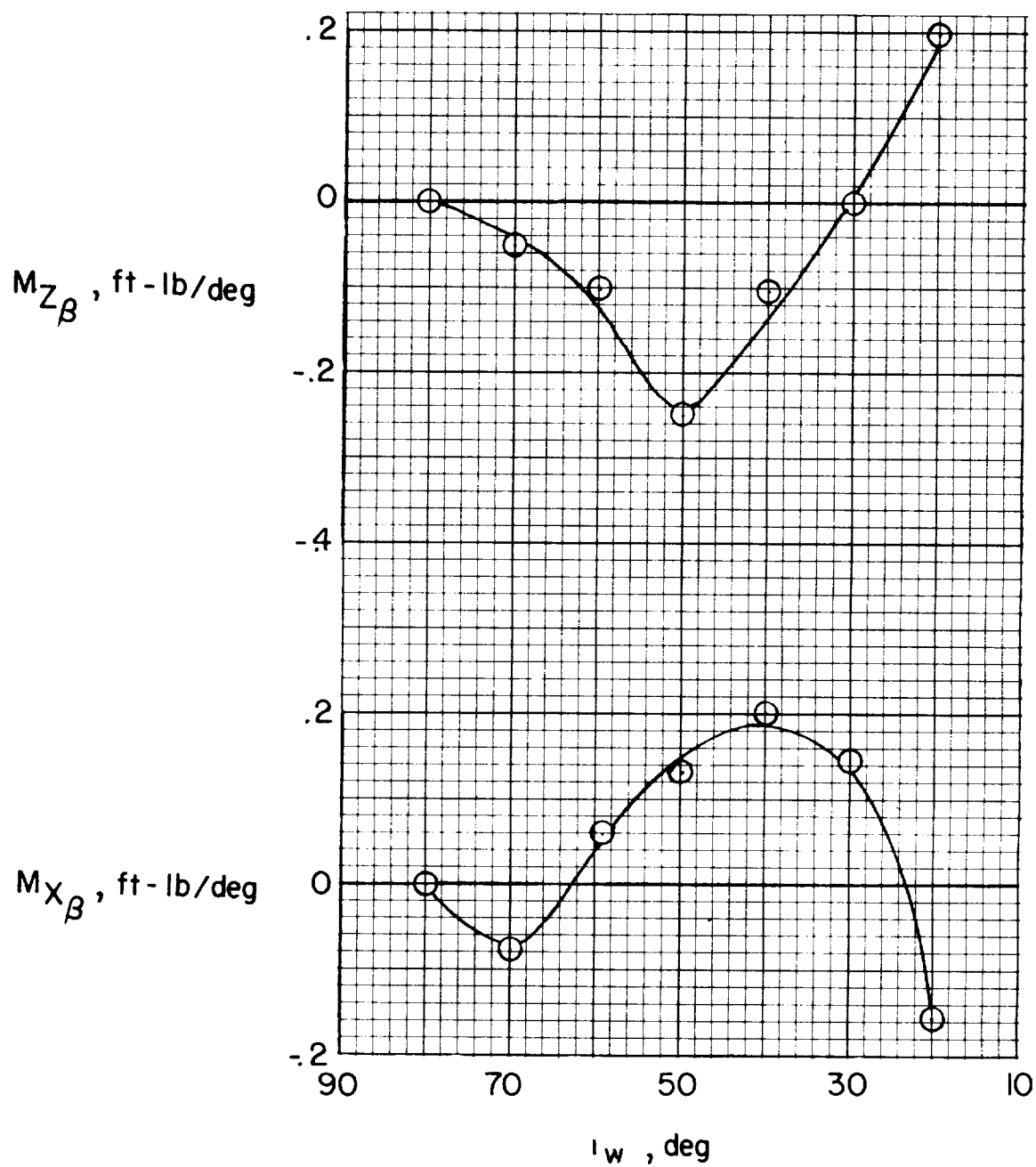


Figure 15.- Variation of directional stability and effective dihedral with wing incidence for the full-span-flap configuration. Data from figure 14.

